

**RELIABILITY-BASED DEVELOPMENT OF TORSIONAL STRENGTH EQUATIONS FOR
THE CSA S16 STANDARD**

© By: Aaron Greene

A thesis submitted to The School of Graduate Studies
in partial fulfillment of the requirements for the degree of

Master of Engineering

Faculty of Engineering and Applied Science

Memorial University

October 2021

St. John's

Newfoundland and Labrador

Canada

Abstract

Steel structures are designed to specific governing design codes which have incorporated reliability parameters that predetermine the required target reliability and margin of safety depending on which country the structure is engineered.

The approved steel design codes ensure each structure is designed with the same quality, recommended loading conditions and safety standards for the design life of the structure. In Canada steel structures are governed by the Canadian Standards Association (CSA) and designed to CAN/CSA S16-19 – Design of Steel Structures [1].

The current Canadian steel design standard (CSA S16-19) gives no specific guidance on methodology with respect to torsional design. This thesis proposes a reliability-based method that, subject to further research and approval by experts in the field, could allow the adoption of strength formulas from other sources for use alongside the CSA S16 Standard while maintaining the desired target reliability.

A series of reliability analyses are performed first to verify the target reliabilities of both the CSA S16 Standard and the AISC 360 specification. Then, an iterative reliability-based approach is used to calibrate the proposed strength formulas in accordance with the desired target reliability of the CSA S16 standard.

Updated resistance factors are then recommended for use with the AISC 360 torsional strength formula for round and rectangular HSS sections so that they can be adopted for use by the CSA S16 standard while maintain the appropriate target reliability index.

Acknowledgements

I would like to thank Dr. Stephen Bruneau and Dr. Amgad Hussein for their input, guidance and recommendations on this thesis. Without their invaluable contribution completion of this thesis would not have been possible.

Table of Contents

Chapter 1. Introduction.....	1
1.1. Background of Study.....	1
1.2. Purpose of Study	1
1.3. Verification Scheme.....	2
1.4. Main Findings	3
Chapter 2. Review of Literature	4
2.1. Comparison of the CSA S16 Standard and the AISC 360 Specification.....	4
2.2. Target Reliabilities of the CSA S16 Standard and the AISC 360 Specification.....	5
2.3. Gap Analysis of the CSA S16 Standard and the AISC 360 Specification.....	9
2.4. Torsional Strength Design of Steel Sections.....	11
2.5. Summary	17
Chapter 3. Reliability and LRFD Background.....	19
3.1. Load and Resistance Factor Design (LRFD)	19
3.2. Principle of Reliability Analysis	20
3.3. Description of Loads	23
3.3.1. Dead Load.....	23
3.3.2. Live Load.....	23
3.3.3. Wind Load	24

3.3.4.	Snow Load	24
3.4.	CSA S16 Statistical Parameters	25
3.4.1.	Resistance	25
3.4.2.	Dead Load	26
3.4.3.	Live Load	27
3.4.4.	Wind Load	29
3.4.5.	Snow Load	31
3.5.	AISC 360 Statistical Parameters	34
3.5.1.	Resistance	35
3.5.2.	Dead Load	36
3.5.3.	Live Load	36
3.5.4.	Wind Load	38
3.5.5.	Snow Load	41
Chapter 4.	Reliability Analysis	44
4.1.	Monte Carlo Simulation	44
4.1.1.	General	44
4.1.2.	CSA S16	45
4.1.2.1.	Dead + Live	47
4.1.2.2.	Dead + Live + Wind	50
4.1.2.3.	Dead + Live + Snow	53

4.1.3.	AISC 360	56
4.1.3.1.	Dead + Live	58
4.1.3.2.	Dead + Live + Wind	61
4.1.3.3.	Dead + Live + Snow	62
4.1.4.	Target Reliabilities.....	64
Chapter 5.	Reliability-Based Strength Formula Development.....	66
5.1.	Reliability-Based Strength Formula Model	66
5.2.	Torsional Strength of Round HSS.....	70
5.3.	Torsional Strength of Rectangular HSS	77
Chapter 6.	Conclusion and Recommendations.....	85
6.1.	General	85
6.2.	Results and Discussion.....	86
6.3.	Future Work	86
References	88
Appendix A – Monte Carlo Simulation Sample	92

List of Tables

Table 1 - Statistical Parameters for The Resistance Load Effects In CSA S16.....	25
Table 2 – Statistical Parameters for The Resistance And Load Effects In AISC 360.....	35
Table 3 – Factored Load Combinations.....	45
Table 4 - Factored Load Combinations using Turkstra’s Rule.....	47
Table 5 – Factored Load Combinations.....	57
Table 6 – Factored Load Combinations using Turkstra’s Rule	58
Table 7 – Round HSS Experimental Data	72
Table 8 – Updated Round HSS Experimental Data.....	75
Table 9 – Rectangular HSS Experimental Data.....	79
Table 10 – Updated Rectangular HSS Experimental Data	83

List of Figures

Figure 1 – Comparison of Nominal Shear Strength (Unstiffened Webs) by Galambos (1999).....	4
Figure 2 – Flowchart of Load and Resistance Factor Design as per Galambos [10].....	7
Figure 3 – Concept of the Plastic Model from Ashkinadze [13].....	15
Figure 4 - Moment-torque interaction diagram for class 1 and 2 beams from Driver and Kennedy [14].....	17
Figure 5 - Moment-torque interaction diagram for class 3 beams from Driver and Kennedy [14].....	17
Figure 6 – Frequency Distribution of Resistance (R) and Load Effect (Q).....	21
Figure 7 – Reliability Index in terms of Safety Margin.....	22
Figure 8 – CSA Resistance Bias Frequency Distribution Curve	26
Figure 9 – CSA Dead Load Bias Frequency Distribution Curve.....	27
Figure 10 – CSA Live Load (Max) Bias Frequency Distribution Curve.....	28
Figure 11 – CSA Live Load (Apt) Bias Frequency Distribution Curve	29
Figure 12 – CSA Wind Load (Max) Bias Frequency Distribution Curve	30
Figure 13 – CSA Wind Load (Apt) Bias Frequency Distribution Curve	31
Figure 14 – CSA Snow Load (max) Bias Frequency Distribution Curve	33
Figure 15 – AISC Resistance Bias Frequency Distribution Curve.....	35
Figure 16 – AISC Live Load Bias Frequency Distribution Curve	37
Figure 17 – AISC Live Load (Apt) Bias Frequency Distribution Curve.....	38
Figure 18 – CSA Wind Load (Max) Bias Frequency Distribution Curve	40
Figure 19 – CSA Wind Load (Apt) Bias Frequency Distribution Curve	41
Figure 20 – CSA Snow Load (Max) Bias Frequency Distribution Curve.....	42

Figure 21 – AISC Snow Load (Apt) Bias Frequency Distribution Curve.....	43
Figure 22 – Frequency Distributions For Random Values of Q and R with L/D = 3.0.....	49
Figure 23 – CSA Reliability Indices for DL + LL and $\phi=0.9$	50
Figure 24 - CSA Reliability Indices for DL + LL and varying ϕ	50
Figure 25 – CSA Reliability Indices for DL + LL + WL	51
Figure 26 – CSA Reliability Indices for DL + LL + WL with W/D = 0.25	52
Figure 27 – CSA Reliability Indices for DL + LL + WL with W/D = 1.0	52
Figure 28 – CSA Reliability Indices for DL + LL + WL with W/D = 2.0	53
Figure 29 – CSA Reliability Indices for DL + LL + WL with W/D = 3.0	53
Figure 30 – CSA Reliability Indices for DL + LL + SL.....	54
Figure 31 – CSA Reliability Indices for DL + LL + SL with S/D = 0.25	55
Figure 32 – CSA Reliability Indices for DL + LL + SL with S/D = 1.0	55
Figure 33 – CSA Reliability Indices for DL + LL + SL with S/D = 2.0	56
Figure 34 – CSA Reliability Indices for DL + LL + SL with S/D = 3.0	56
Figure 35 – Frequency Distributions For Random Values of Q and R with L/D = 3.....	59
Figure 36 – AISC Reliability Indices for DL + LL and $\phi=0.9$	60
Figure 37 – AISC Reliability Indices for LL + DL and Varying ϕ	60
Figure 38 – AISC Reliability Indices for DL + LL + WL with W/D = 0.25.....	61
Figure 39 – AISC Reliability Indices for DL + LL + WL with W/D = 1.0.....	61
Figure 40 – AISC Reliability Indices for DL + LL + WL with W/D = 2.0.....	62
Figure 41 – AISC Reliability Indices for DL + LL + WL with W/D = 2.0.....	62
Figure 42 – AISC Reliability Indices for DL + LL + SL with S/D = 0.25	63
Figure 43 – AISC Reliability Indices for DL + LL + SL with S/D = 1.0.....	63

Figure 44 – AISC Reliability Indices for DL + LL + SL with S/D = 2.0	64
Figure 45 – AISC Reliability Indices for DL + LL + SL with S/D = 3.0	64
Figure 46 – Reliability-Based Strength Formula Model.....	69
Figure 47 – Frequency Distribution Curve of Round HSS using AISC strength formula	73
Figure 48 – Reliability Index Graph for Round HSS using AISC strength formula	73
Figure 49 – Nominal Torsional Strength of Round HSS Members – AISC 360 and Proposed CSA S16	75
Figure 50 - Reliability Index Graph for Round HSS using Proposed CSA strength formula	76
Figure 51 – Frequency Distribution Curve of Rectangular HSS using AISC strength formula...	80
Figure 52 – Reliability Index Graph for Rectangular HSS using AISC strength formula	81
Figure 53 – Nominal Torsional Strength of Rectangular HSS Members – AISC 360 and Proposed CSA S16.....	82
Figure 54 - Reliability Index Graph for Rectangular HSS using Proposed CSA strength formula	83

Chapter 1. Introduction

1.1. Background of Study

Both Canada and the United States have adopted the LRFD approach for design of steel structures. Canadian steel building design currently is governed by the CAN/CSA S16 Design of Steel Structures [1], while the United States steel building design makes use of ANSI/AISC 360-16 - Specification for Structural Steel Buildings [2]. Despite the similar approaches used by each code, there are differences in terms of clauses available in each. Some strength calculations in the CSA S16 Standard have less guidance (or none at all) than is provided in the AISC 360 Specification, for example, torsional strength of steel sections.

Detailed comparison of the two standards have been made in the past, for example, by Galambos [3]. Galambos found that the codes were similar enough in most areas that there appears to be no major obstacle to arriving at mutually satisfactory codes which are essentially interchangeable among countries.

To promote the interchangeability of codes and standards between countries, it is first important to establish appropriate design guidelines and resistance factors that are consistent with the philosophy of the steel design codes.

1.2. Purpose of Study

The goal of this thesis is to expand on this idea by proposing a reliability-based model of adopting torsional strength equations for use with the CSA S16 Standard and load factors and combinations specified in the National Building Code of Canada. This thesis is focused on torsional strength

equations, but the proposed model could be used to adopt any desired strength equation for use with the CSA S16 Standard.

An established method of adopting strength formulas from other sources for use in the CSA S16 Standard would benefit engineers by allowing more flexibility and options when designing steel structures.

The strength clauses used in the AISC 360 Specification, other LRFD based codes, and the CSA S16 Standard are very similar in many cases. However, if the target reliabilities of the codes are not the same, then the formulas cannot be used interchangeably. To adopt the use of strength formulas from other sources for use in the CSA S16 standard, it is important to establish appropriate design guidelines and resistance factors to be used which will ensure the proper target reliability recommended by the CSA Standards Committee.

This thesis proposes a reliability-based method that, subject to further research and approval by experts in the field, could allow the adoption of strength formulas from other sources for use alongside the CSA S16 Standard while maintaining the desired target reliability. The focus of this thesis is the AISC 360 torsional strength formulas for round HSS and rectangular HSS sections due to the clear gap in the CSA S16 standard.

1.3. Verification Scheme

In this thesis, a series of reliability analyses have been conducted to verify the target reliabilities of both the CSA S16 Standard and the AISC 360 specification. Then, an iterative reliability-based approach has been used to calibrate proposed strength formulas in accordance with the desired target reliability of the CSA S16 standard. Strength formulas for both round HSS and rectangular HSS sections are proposed.

Analysis has been performed using the Monte Carlo Simulation method and well-established probabilistic resistance and load models obtained from the available sources used by both standards.

1.4. Main Findings

The main findings of this thesis are that both the AISC 360 torsional strength formula for round HSS sections, as well as the AISC 360 torsional strength formula for rectangular HSS sections can be adopted into the CSA S16 standard, if appropriate resistance factors are applied to ensure the desired target reliability of the CSA S16 Standard is maintained.

The AISC 360 torsional strength formula for round HSS sections can be adopted into the CSA S16 standard with a resistance factor $\phi = 1.0$. This corresponds to a 10% increase in capacity from the AISC formula while still maintaining the desired target reliability for the CSA S16 standard.

The AISC 360 torsional strength formula for rectangular HSS sections can be adopted into the CSA S16 standard with a resistance factor $\phi = 0.75$. This corresponds to a 17% reduction in capacity from the AISC formula while still maintaining the desired target reliability for the CSA S16 standard.

Chapter 2. Review of Literature

2.1. Comparison of the CSA S16 Standard and the AISC 360 Specification

The design of structures is regulated by building codes. The AISC 360 Specification and the CSA S16 Standard were compared by Galambos in 1999 [3]. This comparison explored plate slenderness limits, column curves, web shear capacity, laterally unsupported wide-flange beams, and beam-columns. Detailed comparisons and graphs were made comparing the strength formulas of each code. An example of one of the comparison graphs is shown in Figure 1. This shows a comparison of the nominal shear strength provided by each code, where the shear strength calculated according to CSA S16 Standard is slightly higher for a range of h/t_w than that provided by the AISC 360 Specification.

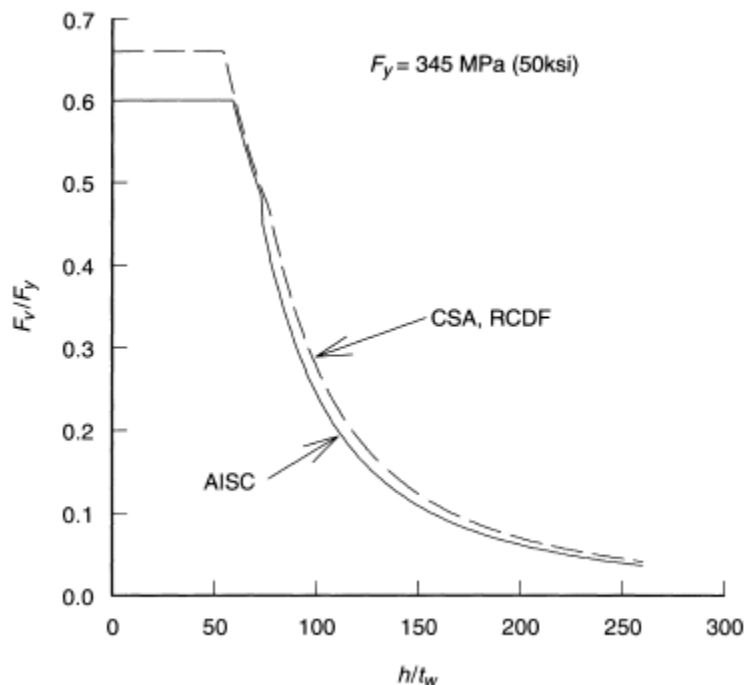


Figure 1 – Comparison of Nominal Shear Strength (Unstiffened Webs) by Galambos (1999)

Galambos found that while the theoretical and experimental basis for all three codes is common, in many cases the final form of the criteria is not the same: different formulas are used for columns, beams, and beam-columns. However, Galambos determined that there appears to be no major obstacle to arriving at mutually satisfactory codes which are essentially interchangeable among countries. This is an interesting idea which would offer benefits to both countries. Normally, the resistance of structural members is expressed in terms of formula(s) that are founded on experiments, theory, or a combination of both. However, it would be useful to allow strength formulas to be adapted from another code. It should be noted that the work of Galambos did not compare the target reliabilities and compatibilities of each code, and did not examine gaps where some strength clauses present in one code might be absent from another.

2.2. Target Reliabilities of the CSA S16 Standard and the AISC 360 Specification

In order to use the design codes of two countries interchangeably, as mentioned by Galambos, the target reliabilities of each code must first be examined. This was not addressed by Galambos in Ref [3], however, we can examine it here.

Structural standards for buildings in Canada moved toward a limit states philosophy in 1974 when a study was released by D.E. Allen [4]. This thesis introduced limit states design partial safety factors in an effort to give more consistent safety for various load combinations and various combinations of materials.

Later, with the release of the 2005 edition of the National Building Code of Canada (NBCC) came the adoption of a companion-action format for load combinations. A paper by Bartlett et al [5] [6], presented the calibration of the new factors required in order to maintain a target reliability index

of 3.0 for members. Probabilistic methods were used to establish the statistical parameters for resistance, dead load, live load, wind load, and snow load used in this thesis.

Similarly, structural standards for buildings in the United States started to move toward a limit states philosophy based on probabilistic methods in 1978 with the work of Ellingwood et al [7]. This work established statistical parameters for resistance, dead load, live load, wind load, and snow load and was used to develop the recommended load combinations for inclusion in ANSI Standard A58 [8], which later became the ASCE7 Standard [9].

In 1980, Galambos [10] further examined load and resistance factor design and recommended load/resistance factors to be used in ANSI Standard A58 [8]. In this study, Galambos outlined the probabilistic methodology for determination of reliability index, providing the following formula:

$$\beta = \frac{\ln(R_m/Q_m)}{\sqrt{V_R^2 + V_Q^2}} \quad (2-1)$$

R_m = mean value of the resistance, R

Q_m = mean value of the load effect, Q

V_R = coefficient of variation of the resistance, R

V_Q = coefficient of variation of the load effect, Q

The study also proposes the following flowchart for load and resistance factor development:

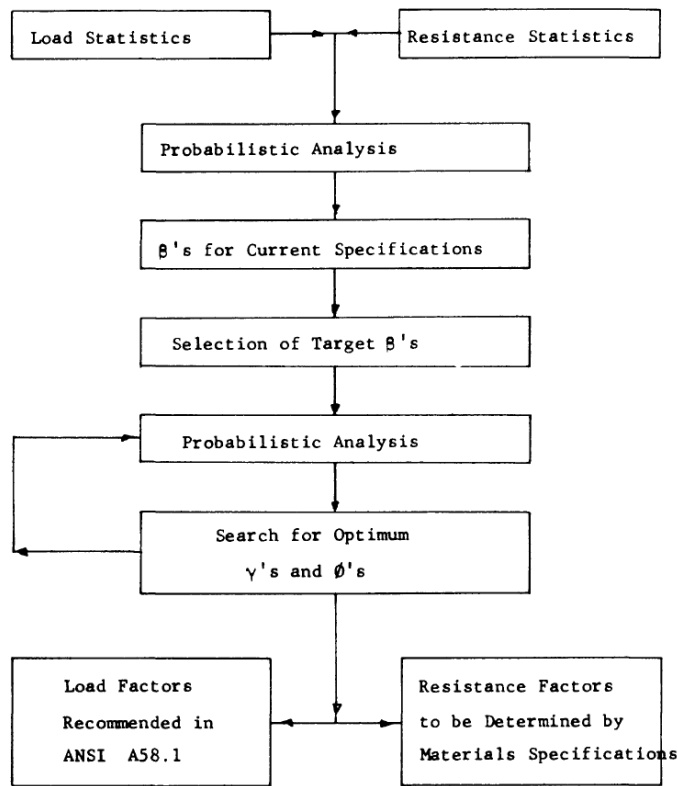


Figure 2 – Flowchart of Load and Resistance Factor Design as per Galambos [10]

Galambos recommended that a resistance factor of 0.85 be adopted by AISC for designing members to achieve a reliability index of 3.0. However, the current AISC 360 specification commentary uses a resistance factor of 0.9 and reports a target reliability of 2.6 for members [2].

It is difficult to recommend using clauses and strength formulas interchangeably between countries without some consideration to difference in target reliabilities. However, it may be possible to adapt formulas between each with some modifications and consideration of target reliabilities and natural variations in material properties, fabrication tolerances and deviation of the model from experimental outcomes. To achieve this a reliability-based method of establishing strength formulas must be used.

The North American Specification for the Design of Cold-Formed Steel Structural Members [11] establishes a reliability-based method for developing strength formulas from test data. The average strength value from the test data is used, and a resistance factor is calculated based on the desired target reliability, and the biases and coefficients of variation of the test data and mechanical properties of the steel. The strength of the tested elements shall satisfy:

$$\sum \gamma_i Q_{in} \leq \phi R_n \quad (2-2)$$

Where:

γ_i = load factor applicable to a specific load component

Q_{in} = a specific nominal load component

$\sum \gamma_i Q_{in}$ = the total factored load for the load group applicable to the limit state being considered

R_n = the average value of all test results

ϕ = the resistance factor = $C_\phi (M_M F_M P_M) e^{-\beta_o \sqrt{V_M^2 + V_F^2 + C_P V_P^2 + V_Q^2}}$

C_ϕ = calibration coefficient

M_M = mean value of material factor

F_M = mean value of fabrication factor

P_M = mean value of professional factor

β_o = target reliability index

V_M = coefficient of variation of material factor

V_F = coefficient of variation of fabrication factor

V_P = correction factor

V_P = coefficient of variation of professional factor

V_P = coefficient of variation of load effect

This method is comprehensive, and useful when testing is an option or test data already available.

However, it is not so useful when test data is not available for the specific section being designed,

and performing tests is not practical. In that case, it would be of benefit to have a reliability-based method of adapting strength formulas from one code to another without having to test the specific section or element in question.

A reliability-based method of developing strength equations was used by Leblouba and Tabsh [12] to develop shear strength equations for corrugated web steel beams for inclusion in the AISC 360 Specification and the CSA S16 Standard. This study proposed adapting nominal buckling strength capacity equations of corrugated web steel beams with consideration of reliability-based design for use in LRFD codes while maintaining desired target reliabilities.

This study confirms the difference in reliability indices between the two codes, as a slightly different resistance factor is recommended to be used depending on the code (0.9 For CSA S16, and 0.85 for AISC 360). The study is focused on the shear strength of corrugated web steel beams only, however, with some modifications this method could also be used to aid in developing a method to allow strength formulas to be used interchangeably between the AISC 360 Specification and the CSA S16 Standard.

2.3. Gap Analysis of the CSA S16 Standard and the AISC 360 Specification

The AISC 360 Specification [2] and the CSA S16 Standard [1] were examined in detail to identify gaps between the two to identify potential benefits of allowing interchangeability between the two codes. Some of the major differences noted include:

Tension

- Differences in constants used in effective area calculations for shear lag.
- More shear lag factor cases covered in AISC for connections to tension members, ie HSS with 2 side gusset plates.

- No guidance on eyebars provided by the CSA S16 Standard.

Compression

- Differences in width to thickness limits.
- Differences in constants throughout.

Flexure

- Difference in codes in that AISC checks local buckling of elements, and CSA limits section sizes with classes in order to prevent local buckling.
- Compression flange buckling not specifically checked, or flange local buckling under weak axis bending, however the classes of sections are limited to prevent this.
- Lateral torsional buckling of rectangular and round bars not checked under CSA.

Shear

- Differences throughout codes in calculating shear buckling coefficients. Differences in constants, in general 0.6 used in AISC, and 0.66 in CSA.
- CSA S16 offers no real guidance for shear on Tees, and zero on angles. Can check basic shear yielding of these, but no guidance on shear buckling.
- CSA S16 verifies shear yielding of HSS members, however, does not consider the effects of shear buckling of HSS members with large D/t ratios.
- No guidance in CSA on weak axis shear. It is assumed flange areas would be used in calculating shear yielding, but no guidance on shear buckling coefficients or factors.

Torsion

- No guidance provided in CSA S16. Torsional strength calculations are provided for round and rectangular HSS sections in AISC, as well as combined torsional, axial, and flexure, and shear.

The focus of this thesis is on torsional strength, as the clear gap in the CSA S16 Standard makes it a good starting point.

2.4. Torsional Strength Design of Steel Sections

The AISC 360 Specification provides strength formulas for Round HSS and Rectangular HSS sections. The formulas consider yielding as well as local buckling. The AISC 360 Specification assumes that the pure torsional shear stress in HSS sections is uniformly distributed along the wall of the cross section, and it is equal to the torsional moment divided by a torsional shear constant for the cross section, C .

The strength equation for round HSS sections given by AISC 360 is as follows:

$$T_n = F_{cr} C \quad (2-3)$$

Where:

$$C = \text{HSS Torsional Constant} = \frac{\pi(D - t)^2 t}{2}$$

and F_{cr} shall be the larger of:

$$F_{cr} = \frac{1.23E}{\sqrt{\frac{L}{D} \left(\frac{D}{T}\right)^{\frac{5}{4}}}} \quad (2-4)$$

and:

$$F_{cr} = \frac{0.60E}{\left(\frac{D}{t}\right)^{\frac{3}{2}}} \quad (2-5)$$

and shall not exceed:

$$F_{cr} = 0.6F_y$$

The strength equation for rectangular HSS sections given by AISC 360 is as follows:

$$T_n = F_{cr}C \quad (2-6)$$

Where:

$$C = \text{HSS Torsional Constant} = 2(B - t)(H - t)t - 4.5(4 - \pi)t^3$$

When $h/t \leq 2.45\sqrt{E/F_y}$:

$$F_{cr} = 0.6F_y \quad (2-7)$$

When $2.45\sqrt{E/F_y} < h/t \leq 3.07\sqrt{E/F_y}$:

$$F_{cr} = \frac{0.6F_y(2.45\sqrt{E/F_y})}{\left(\frac{h}{t}\right)} \quad (2-8)$$

When $3.07\sqrt{E/F_y} < h/t \leq 260$:

$$F_{cr} = \frac{0.458\pi^2 E}{\left(\frac{h}{t}\right)^2} \quad (2-9)$$

The critical torsional stress provisions for HSS sections are identical to the flexural shear provisions. As such, the differences in shear formulas between AISC 360 and CSA S16 may be useful in proposing torsional strength formulas to be used in CSA S16.

While normal and shear stresses due to restrained warping are insignificant in closed cross sections, they are usually significant in shapes of open cross section. In HSS sections the total torsional moment can be assumed to be resisted by pure torsional shear stresses. This makes the torsional strength formulas for Round and Rectangular HSS sections easier to determine and maintain in a code, however, for open sections the AISC 360 specifications, like the CSA S16 Standard, gives no guidance.

In terms of open sections, formulas have been proposed for torsional strength of wide-flange steel members by Ashkinadze [13] in 2008. The paper addresses the design of wide-flange members subjected to torsional forces as well as axial forces and moments about their strong and weak axes.

Ashkinadze proposes a plastic model for use with Class 1 sections, and an elastic model for use with class 2 and class 3 sections. The plastic model originated from the internal stress distribution in an I-section subjected to flexure and torsion proposed by Driver and Kennedy [14]. The proposed plastic model Ashkinadze is as follows:

$$M_f = \phi F_y t a (b - a) \quad (2-10)$$

Where t and b are standard designations for the thickness and width of the flange, respectively. Solving for a determines how much of the flange width is claimed by torsion and unusable to resist other forces. To solve for a , Ashkinadze proposes the following formulas to aid in solving for a :

$$B = M_f h' \quad (2-11)$$

and

$$B = EC_w \theta'' \quad (2-12)$$

Where B is the bi-moment caused by the torsional loads, C_w is the warping stiffness of the section, h' is the distance between the centroids of the flanges, E is the modulus of elasticity of the steel, and θ'' is the second derivative of the angle of twist.

Once the length of a has been determined, the end segments are excluded from consideration and the rest of the section is analyzed for the remaining axial and bending forces by the usual equations of the CSA S16 standard as shown in Figure 3.

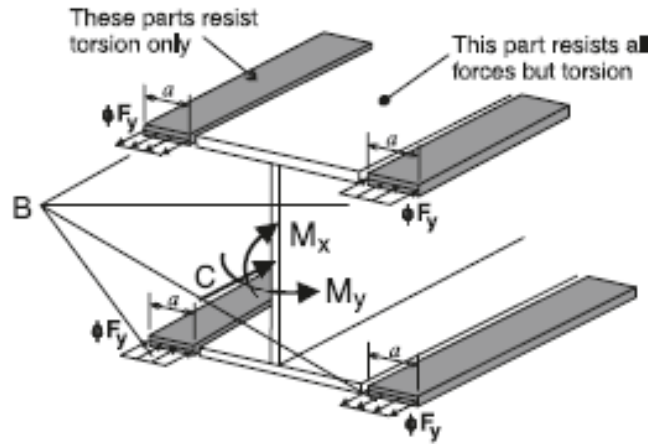


Figure 3 – Concept of the Plastic Model from Ashkinadze [13]

The elastic model proposed by Ashkinadze is derived from the following formula from AISC 360 [2]

$$\frac{\sigma_a}{8.85F_{cr}} \pm \frac{\sigma_{bx}}{(1 - P_u/P_{ex})\phi_b F_{cr}} \pm \frac{\sigma_{by}}{(1 - P_u/P_{ey})0.9F_y} \pm \frac{\sigma_w}{(1 - P_u/P_{ey})0.9F_y} \leq 1.0 \quad (2-13)$$

This equation is modified to include integral force factors rather than stresses, and modified further using basic torsional theory to produce the following proposed equation:

$$\frac{C_f}{C_r} + \frac{U_{1x}M_{fx}}{M_{rx}} + \frac{1}{1 - M_{fx}/M_u} \left(\frac{U_{1y}M_{fy}}{M_{ry}} + \frac{U_{1y}\sigma_w Z_y}{M_{ry}} \right) \leq 1.0 \quad (2-14)$$

Ashkinadze compares his proposed equations to test results from Driver and Kennedy [14] and Pi and Trahair [15] and concludes that the model gives results that are reasonable, however recommends more rigorous verification against test data and detailed non-linear second-order

computer simulations. Ashkinadze's study was limited to simply supported members of symmetrical I-sections.

Ashkinadze's work was built on the work of Pi and Trahair [15], who examined the plastic-collapse analysis of structural steel I-sections members subjected to torsion. Most previously accepted methods of torsion design in beams, such as those based on the work of Timoshenko [16], are based on the theory of first yield, and therefore don't take into account plastic behavior. The paper proposes a method of plastic-collapse analysis that is claimed to be simpler than elastic analysis. This plastic-analysis method allows a method of plastic design to be used for torsion that is more economical than first yield design. It was proposed that this will lead to more economical section design. Only compact I-section members that have no local buckling limitations are considered in this study.

Ashkinadze also refers to the work of Driver and Kennedy [14], which aimed to investigate the behavior torsional capacity of members. The paper notes that prior literature on elastic analysis is extensive, but only limited experimental and analytical work has been conducted in the inelastic region. It further states that methods for determining the ultimate capacity, as is required in limit states design standards, are not available.

Driver and Kennedy perform testing on cantilever beams with varying moment-torque ratios to investigate torsional behavior in the inelastic range.

Driver and Kennedy developed the moment-torque interaction diagrams shown in Figure 4 and Figure 5.

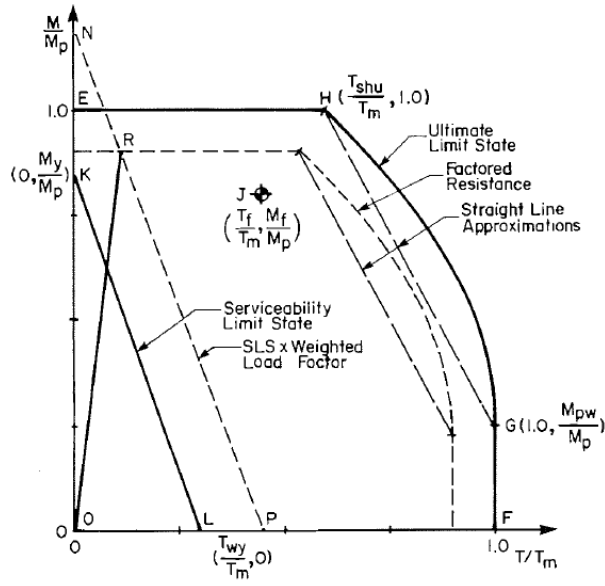


Figure 4 - Moment-torque interaction diagram for class 1 and 2 beams from Driver and Kennedy [14]

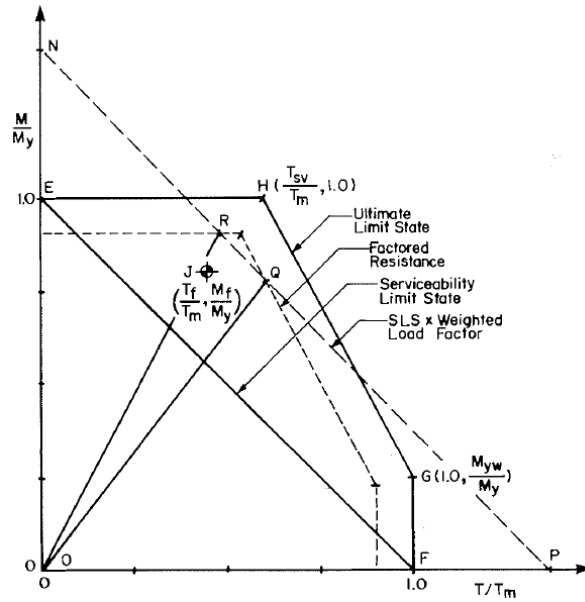


Figure 5 - Moment-torque interaction diagram for class 3 beams from Driver and Kennedy [14]

2.5. Summary

Significant research and development has gone into developing a limit states based approach for the CSA S16 standard which gives consistent safety for various load combinations and various

combinations of materials. Probabilistic methods were used to establish the statistical parameters for resistance, dead load, live load, wind load, and snow load and to provide the desired reliability index for the standard.

The North American Specification for the Design of Cold-Formed Steel Structural Members [11] establishes a reliability-based method for developing strength formulas from test data, however, there does not appear to be an established reliability-based model to adopt strength formulas from other codes and sources.

Chapter 3. Reliability and LRFD Background

3.1. Load and Resistance Factor Design (LRFD)

In the 1960's and 70's, a push was made in the United States and Canada to adopt the LRFD approach. Prior to this, Allowable Stress Design (ASD) was widely used. While simple to use, the ASD method was found to give less consistent target reliability than an LRFD approach. This was due in part to the same factor being applied to dead load, which is relatively predictable, and live/wind/snow loads, which are much more variable. The variation in reliability was reduced substantially upon the adoption of an LRFD approach, which in turn leads to more optimized designs.

The following basic equation can be used to represent limit states design:

$$\sum \gamma_i Q_{in} \leq \phi R_n \quad (3-1)$$

where:

γ_i = load factor applicable to a specific load component

Q_{in} = a specific nominal load component

$\sum \gamma_i Q_{in}$ = the total factored load for the load group applicable to the limit state being considered

ϕ = the resistance factor

R_n = the nominal resistance available

A limit state is a condition, related to a design objective, in which a combination of one or more loads is just equal to the available resistance, so that the structure is at incipient failure defined by a prescribed failure criterion (or deformed beyond an acceptable prescribed amount).

Load and resistance factors in Equation (3-1) are used to account for material variability, uncertainty in magnitude of the applied loads, design models, and other sources. The objective in LRFD is to ensure that for each limit state the available resistance is at least as large as the total load effect.

Equation (3-1) is the design equation, but it can serve as the basis for the development of a limit state equation that can be used for calibration purposes. If there is only one load component, Q_n , then Equation (3-1) can be shown as:

$$\phi R_n - \gamma Q_n \geq 0 \quad (3-2)$$

where

R_n = the nominal resistance value;

Q_n = the nominal load value;

ϕ = a resistance factor; and

γ = a load factor

This equation forms the basis for the reliability analysis equations discussed in the following section.

3.2. Principle of Reliability Analysis

Reliability analysis is a probabilistic approach to determine the safety level of a system or a structure. Structural reliability aims at computing the probability of failure of a mechanical system by accounting for uncertainties arising in a model description (geometry, material properties) or in the environmental data (prescribed displacement and external forces).

Frequency distributions for R and Q are shown in Figure 6 as separate curves. As long as the resistance (R), is greater than the effects of the loads (Q), a margin of safety for the particular limit state exists. However, because R and Q are random variables affected by many uncertainties, there is always a probability that R may be less than Q. This probability of failure is represented by the overlap of the frequency distributions. The size of this overlap (and thus the probability of failure P_f) is dependent on the positioning of their mean values (R_m and Q_m) and their dispersions, or coefficients of variation (V_R and V_Q).

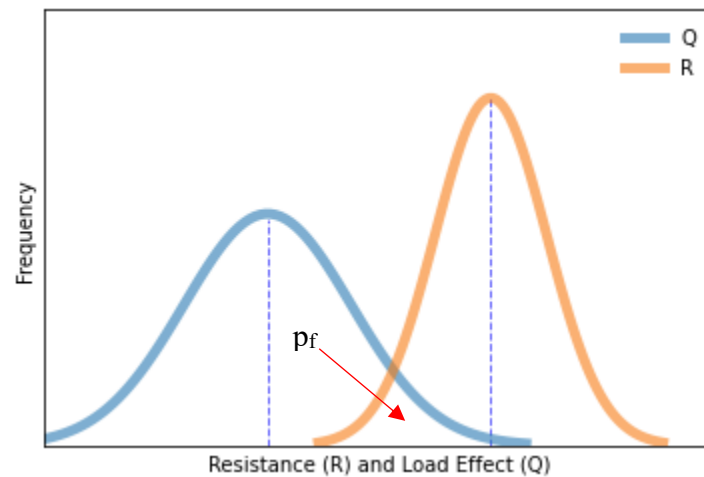


Figure 6 – Frequency Distribution of Resistance (R) and Load Effect (Q)

The structure failure state can also be defined by a limit state function $g(x) = R - Q$ such that:

$g(x) < 0$ is the failure state for the structure.

$g(x) = 0$ is the limit state.

$g(x) > 0$ is a safe state for the structure.

Therefore, the objective of reliability analysis is to determine the probability of $g(x)$ being negative, aka the probability of failure.

The reliability index (β) is the distance between the mean of $g(x)$ and the failure point in standard deviation units. As such, β is a measure of the probability that $g(x)$ will be less than zero. This is represented in Figure 7.

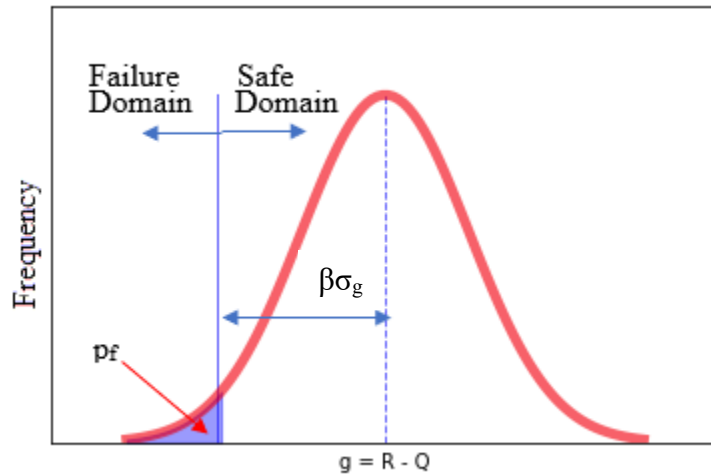


Figure 7 – Reliability Index in terms of Safety Margin

The probability that $g(x)$ is less than zero depends on the distributions of the many variables that go into computing resistance and load effects, which are discussed in Sections 3.4 and 0.

The reliability index can be calculated using the following formula [7]:

$$\beta = \frac{\ln(R_m/Q_m)}{\sqrt{V_R^2 + V_Q^2}} \quad (3-3)$$

R_m = mean value of the resistance, R

Q_m = mean value of the load effect, Q

V_R = coefficient of variation of the resistance, R

V_Q = coefficient of variation of the load effect, Q

Before proposing a reliability-based model for adopting strength formulas from one code into another, it is useful to verify the target reliability (β) of each code. In order to determine β we must first determine R_m , Q_m , V_R , and V_Q . These can be obtained through Monte Carlo Simulations using the statistical parameters of R and Q . This process is detailed in Section Chapter 4.

3.3. Description of Loads

The following typical loads are examined, which are considered the most typical loads applicable to building design from the North American perspective (CSA and AISC): Dead Load, Live Load, Snow Load, and Wind Load.

3.3.1. Dead Load

Dead load is the self-weight of the structure and any additional superimposed load that is permanently attached to the structure. This includes the weight of the members, the supported structure, and any permanent attachments or accessories. In this thesis, dead load is assumed to remain constant throughout the life of the structure. The bias factor (mean-to-nominal ratio) used in both AISC and CSA statistical parameters suggests that there is a tendency on structural engineers to underestimate the dead load slightly.

3.3.2. Live Load

In building structures, live loads include any temporary or transient forces that act on a building or structural element. Typically, this includes people, furniture, vehicles, moveable partitions and almost everything else that can be moved throughout a building. Total live load is a combination of two components, sustained and temporary. Sustained live load remains relatively constant over a period and is referred to as the arbitrary point in time live load (L_{apt}). Temporary live loads are the uncommon portion of live load that results from rare events such as over-crowding or

remodeling. The maximum live load (L_{max}), is a combination of the sustained and temporary components of the live load.

3.3.3. Wind Load

Wind load effect on building structures depends on many factors including the wind speed, profile, exposure, direction, pressure coefficient, and gust. Like live load, wind load is composed of both an arbitrary point in time wind load (W_{apt}), and a maximum wind load (W_{max}). W_{max} would be characterized by a large bias factor, while W_{apt} is characterized by the daily maximum wind, which has a negligibly small bias factor and large coefficient of variation.

The values of both AISC and CSA statistical parameters for wind load are based on data from multiple sites throughout each relevant country in an effort to provide a broad geographical depiction.

3.3.4. Snow Load

Snow load effect on building structures depends on many factors including climatological records, snow density, roof exposure, roof geometry, and the relationship between snow loads on the roof and snow loads on ground. As above, snow load is composed of both an arbitrary point in time snow load (S_{apt}), and a maximum snow load (S_{max}).

3.4. CSA S16 Statistical Parameters

The statistical parameters of the dead, live, wind, and snow load effects on buildings for the Canadian Standards Association used in this thesis are based on the work of Bartlett et al. [5] [6]. Table 1 shows a summary of the results. The results agree with those used in the calibration of the AISC specification in the case of dead load but deviate in cases of live, wind, and snow loads.

Load	Bias	COV	Distribution	Reference
Resistance (Steel)	1.17	0.108	Lognormal	[6]
Dead Load	1.05	0.10	Normal	[5]
Live Load (max)	0.9	0.267	Gumbel	[5]
Live Load (apt)	0.273	0.705	Weibull	[5]
Wind Load (max)	0.712	0.241	Gumbel	[5]
Wind Load (apt)	0.069	0.980	Weibull	[5]
Snow Load (max)	0.660	0.495	Lognormal	[5]
Snow Load (apt)	0.118	0.992	Lognormal	[5]

Table 1 - Statistical Parameters for The Resistance Load Effects In CSA S16.

3.4.1. Resistance

Resistance is assumed to be characterized by a lognormal probability distribution with a bias factor of 1.17 and a coefficient of variation of 0.108 [5]. The lognormal distribution curve can be generated using the lognorm function from Python's SciPy library. To produce a Lognormal distribution with a bias = 1.17 and COV = 0.108, a shape factor = 0.125, location factor of 0.1622, and a scale factor of 1.0 must be used in the lognorm function. The resulting distribution curve is shown in Figure 8.

x

```
= numpy.linspace(lognorm.ppf(0.001, s, loc, scale), lognorm.ppf(0.999, s, loc, scale), 100)
```

```
matplotlib.pyplot.plot(x, lognorm.pdf(x, s, loc, scale))
```

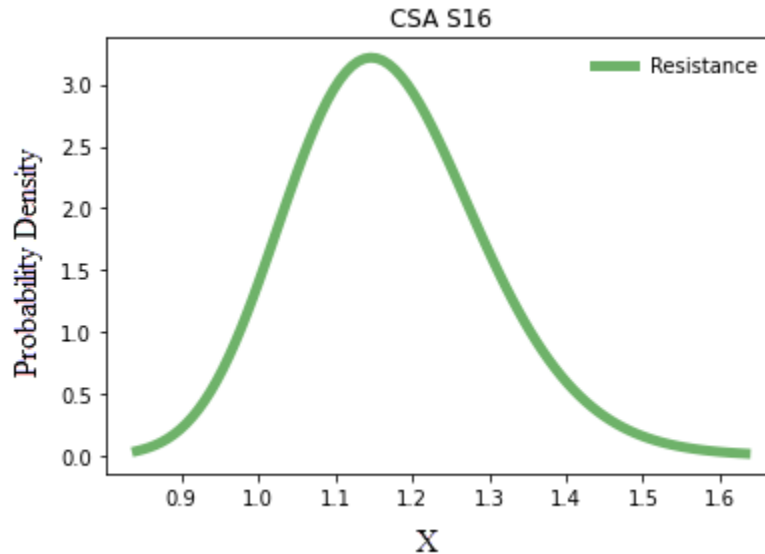


Figure 8 – CSA Resistance Bias Frequency Distribution Curve

3.4.2. Dead Load

The dead load is characterized by a normal probability distribution, with a mean of 1.05 and a COV of 0.1. For cases where the dead load counteracts the effects of other loads, the load is considered unbiased (mean = 1.0). For now, we will only examine the biased case. The normal distribution curve can be generated using the norm function from Python’s SciPy library. To produce a Normal distribution with a bias = 1.0 and c.o.v. = 0.1, a location factor of 0.105, and a scale factor of 0.1 must be used in the norm function. The resulting distribution curve is shown in Figure 9.

```
 $x = \text{numpy.linspace}(\text{norm.ppf}(0.001, \text{loc}, \text{scale}), \text{norm.ppf}(0.999, \text{loc}, \text{scale}), 100)$ 
```

`matplotlib.pyplot.plot(x, norm.pdf(x, loc, scale))`

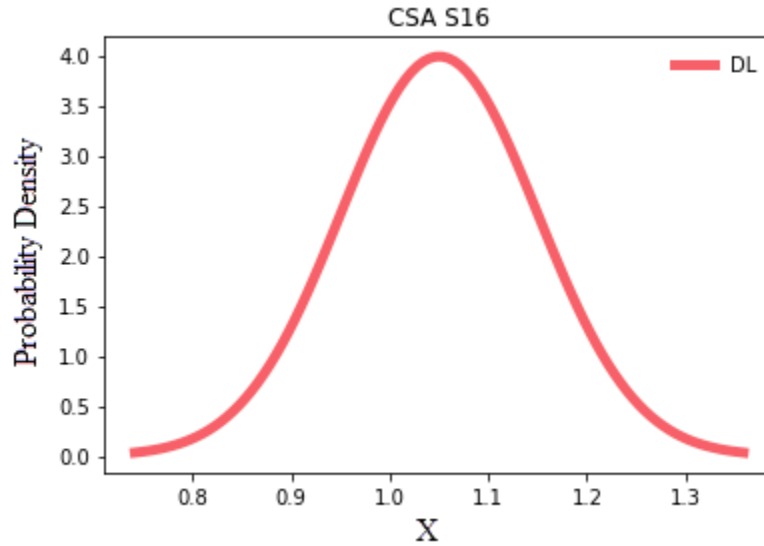


Figure 9 – CSA Dead Load Bias Frequency Distribution Curve

3.4.3. Live Load

The maximum live load during the life of the structure is characterized by a Gumbel probability distribution, with a mean of 0.9 and a COV of 0.267 [5]. As per [5], this is determined by taking the basic Gumbel probability distribution of 0.9 and a COV of 0.17 and applying a transformation factor to account for modelling and analysis factors. This transformation factor is characterized by a normal distribution with a bias of 1.0 and a CoV of 0.206 [5].

The normal distribution curve can be generated using the `gumbel_r` function from Python's SciPy library. To produce a Gumbel distribution with a bias = 0.9 and COV = 0.267, a location factor of 0.793, and a scale factor of 0.188 must be used in the `gumbel_r` function. The distribution curve is shown in Figure 10.

x

```
= numpy.linspace(gumbel_r.ppf(0.001, loc, scale), gumbel_r.ppf(0.999, loc, scale), 100)
```

```
matplotlib.pyplot.plot(x, gumbel_r.pdf(x, loc, scale))
```

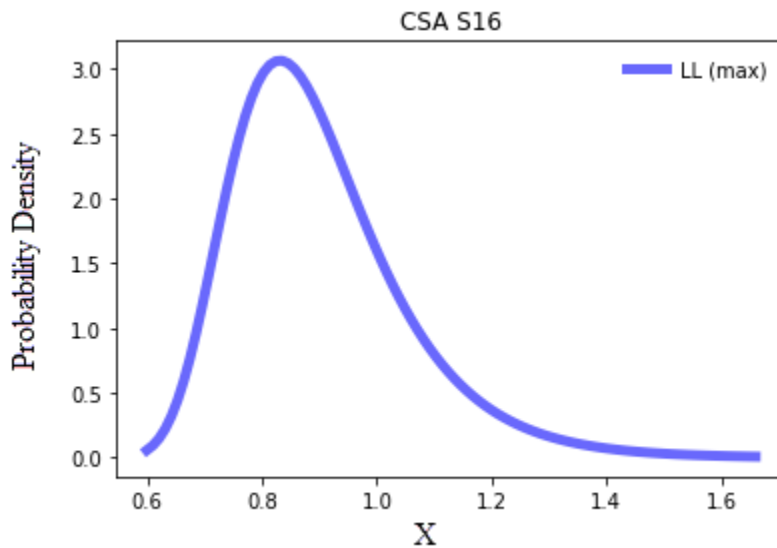


Figure 10 – CSA Live Load (Max) Bias Frequency Distribution Curve

The arbitrary point in time live load is characterized by a Weibull probability distribution, with a mean of 0.273 and a COV of 0.705 [5]. These values have been determined by applying a transformation factor to the load effect which is characterized by a normal distribution with a bias of 1.0 and a CoV of 0.206 [5].

The distribution curve can be generated using the `weibull_min` function from Python's SciPy library. To produce a Weibull distribution with a bias = 0.273 and COV = 0.705, a shape factor of 1.44, location factor of 0, and a scale factor of 0.301 must be used in the `weibull_min` function. The resulting distribution curve is shown in Figure 11.

x

```
= numpy.linspace(weibull_min.ppf(0.001, s, loc, scale), weibull_min.ppf(0.999, s, loc, scale), 100)
```

```
matplotlib.pyplot.plot(x, weibull_min.pdf(x, s, loc, scale))
```

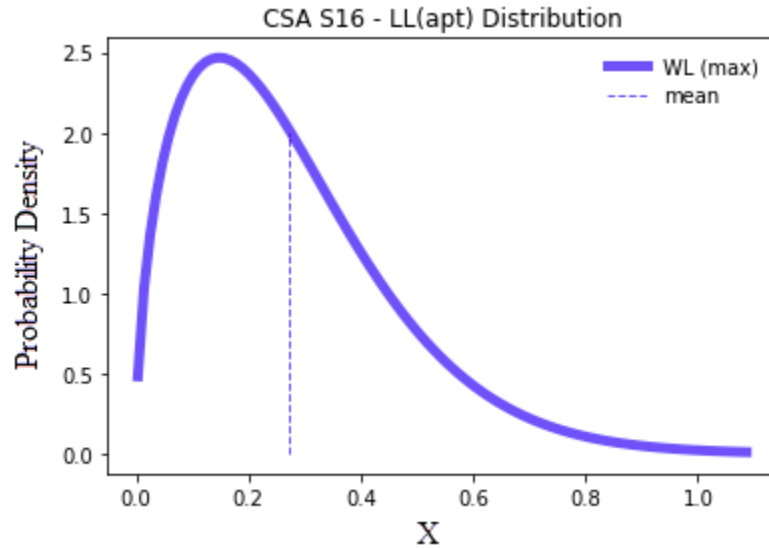


Figure 11 – CSA Live Load (Apt) Bias Frequency Distribution Curve

3.4.4. Wind Load

Wind load data used in reliability analysis in CISC [5] is based on data from three Canadian sites which aims to give a broad geographical representation.

The wind load on a structure is characterized by the following formula:

$$p = q * C_e * C_p * C_g \quad (3-4)$$

where q is the reference velocity pressure, C_e is the exposure factor, C_p is the external pressure coefficient, and C_g is the gust factor. These factors are accounted for by applying a transformation factor to the load effect which is characterized by a lognormal distribution with a bias of 0.68 and a CoV of 0.22 [5].

The maximum wind load during the life of the structure is characterized by a Gumbel probability distribution, with a mean of 0.712 and a COV of 0.241 [5]. This value was found taking the 50-year maximum velocity and applying the transformation factor which accounts for exposure, pressure, and gust factors. The distribution curve can be generated using the `gumbel_r` function from Python's SciPy library. To produce a Gumbel distribution with a bias = 0.712 and COV = 0.241, a location factor of 0.635, and a scale factor of 0.134 must be used in the `gumbel_r` function. The resulting distribution curve is shown in Figure 12.

x

```
= numpy.linspace(gumbel_r.ppf(0.001, loc, scale), gumbel_r.ppf(0.999, loc, scale), 100)
```

```
matplotlib.pyplot.plot(x, gumbel_r.pdf(x, loc, scale))
```

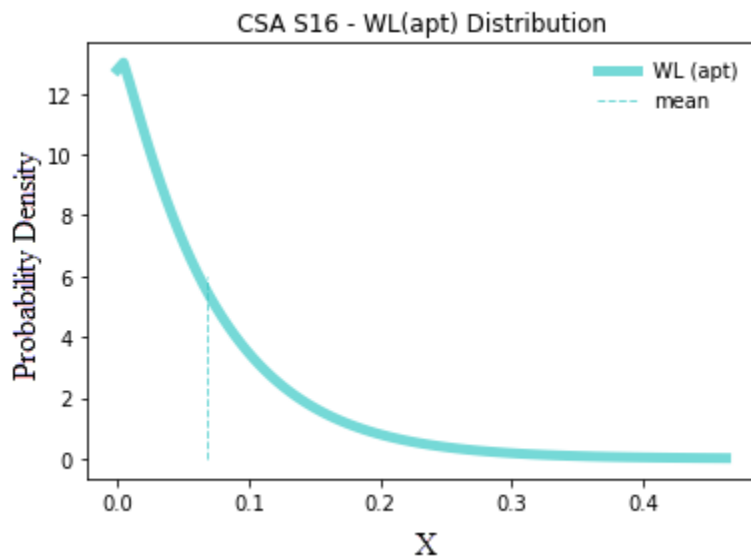


Figure 12 – CSA Wind Load (Max) Bias Frequency Distribution Curve

The arbitrary point in time wind load is characterized by a Weibull probability distribution, with a mean of 0.069 and a COV of 0.98 [5]. These value were found by taking the point in time velocity and applying the transformation factor which accounts for exposure, pressure, and gust factors.

The distribution curve can be generated using the `weibull_min` function from Python's SciPy library. To produce a Weibull distribution with a bias = 0.069 and COV = 0.98, a shape factor of 1.02, location factor of 0, and a scale factor of 0.0696 must be used in the `weibull_min` function. The resulting distribution curve is shown in Figure 13.

x

```
= numpy.linspace(weibull_min.ppf(0.001,s,loc,scale),weibull_min.ppf(0.999,s,loc,scale),100)
```

```
matplotlib.pyplot.plot(x,weibull_min.pdf(x,s,loc,scale))
```

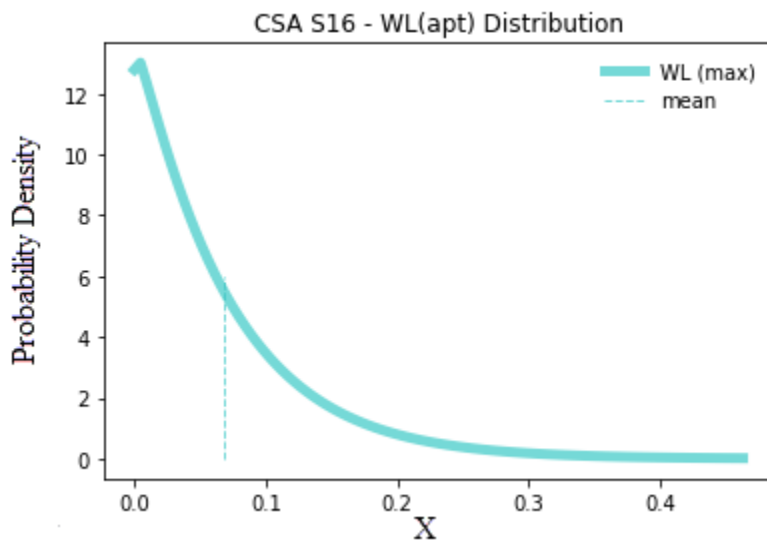


Figure 13 – CSA Wind Load (Apt) Bias Frequency Distribution Curve

3.4.5. Snow Load

Snow load data used in reliability analysis in CISC [5] is based on snow depth data from 1618 stations with 7–38 years of record.

The snow load on a structure is characterized by the following formula:

$$S = (C_b C_w C_s C_a) S_s + S_r \quad (3-5)$$

where S_g is the ground snow load, S_r is the associated rain load, C_b is the basic roof snow load factor and equals 0.8, C_e is the wind exposure factor, C_s is the slope factor, and C_a is the accumulation factor.

The maximum snow load during the life of the structure is characterized by a Lognormal probability distribution, with a mean of 0.66 and a COV of 0.495 [5]. These values were found taking the 50-year maximum depth values (mean = 1.100 and COV = 0.200) and applying a transformation factor (mean = 0.600 and COV = 0.420) which converts the ground snow load at a given site to an appropriate roof snow load. The transformation factor is based on 13 years of data for 112 roofs in four Canadian cities.

The lognormal distribution curve can be generated using the `lognorm` function from Python's SciPy library. To produce a Lognormal distribution with a bias = 1.17 and COV = 0.108, a shape factor = 0.304, location factor of -0.39, and a scale factor of 1.0 must be used in the `lognorm` function. The distribution curve is shown in Figure 8.

x

```
= numpy.linspace(lognorm.ppf(0.001, s, loc, scale), lognorm.ppf(0.999, s, loc, scale), 100)
```

```
matplotlib.pyplot.plot(x, lognorm.pdf(x, s, loc, scale))
```

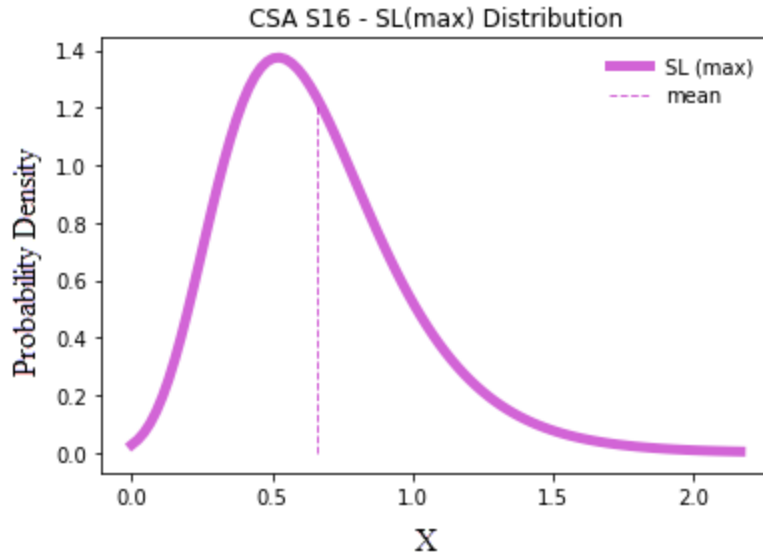


Figure 14 – CSA Snow Load (max) Bias Frequency Distribution Curve

The arbitrary point in time snow load is characterized by a Lognormal probability distribution, with a mean of 0.069 and a COV of 0.98 [5]. This value was found taking the point-in-time values (mean = 0.196 and COV = 0.882) and applying a transformation factor (mean = 0.600 and COV = 0.420) which converts the ground snow load at a given site to an appropriate roof snow load. The distribution curve can be generated using the lognorm function from Python’s SciPy library. To produce a Lognormal distribution with a bias = 0.118 and COV = 0.992, a shape factor of 0.116, location factor of 0, and a scale factor of -0.889 must be used in the lognorm function. The resulting distribution curve is shown in Figure 9.

x

```
= numpy.linspace(lognorm.ppf(0.001, s, loc, scale), lognorm.ppf(0.999, s, loc, scale), 100)
```

```
matplotlib.pyplot.plot(x, lognorm.pdf(x, s, loc, scale))
```

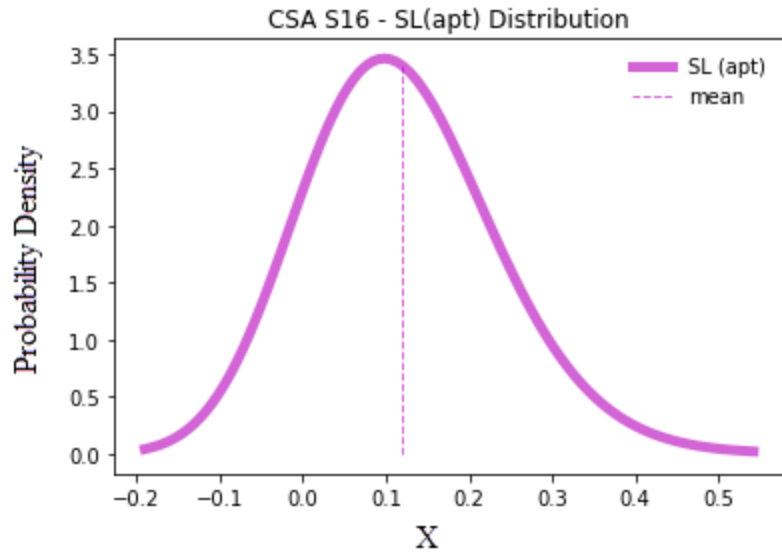


Figure 9 – CSA Snow Load (Apt) Bias Frequency Distribution Curve

3.5. AISC 360 Statistical Parameters

The statistical parameters of the dead, live, wind, and snow load effects on buildings for the American Institute of Steel Construction used in this thesis are based on the work of Ellingwood et. al [7]. Table 2 shows a summary of the results. The results agree with those used in the calibration of the CSA S16 Standard in the case of dead load but deviate in cases of resistance, live, wind, and snow loads.

Load	Bias	COV	Distribution	Reference
Resistance (Steel)	1.10	0.11	Lognormal	[7]
Dead Load	1.05	0.10	Normal	[7]
Live Load (max)	1.0	0.25	Gumbel	[7]
Live Load (apt)	0.24	0.50	Gamma	[7]
Wind Load (max)	0.78	0.37	Gumbel	[7] [17]
Wind Load (apt)	0.01	0.069	Gumbel	[7] [17]

Snow Load (max)	0.82	0.26	Lognormal	[7]
Snow Load (apt)	0.20	0.73	Lognormal	[7]

Table 2 – Statistical Parameters for The Resistance And Load Effects In AISC 360.

3.5.1. Resistance

Resistance is assumed to be characterized by a lognormal probability distribution with a bias factor of 1.10 and a coefficient of variation of 0.11 [7]. The lognormal distribution curve can be generated using the lognorm function from Python’s SciPy library. To produce a Lognormal distribution with a bias = 1.10 and COV = 0.11, a shape factor = 0.121, location factor of 0.095, and a scale factor of 1.0 must be used in the lognorm function. The distribution curve is shown in Figure 15.

```
x
= numpy.linspace(lognorm.ppf(0.001, s, loc, scale), lognorm.ppf(0.999, s, loc, scale), 100)

matplotlib.pyplot.plot(x, lognorm.pdf(x, s, loc, scale))
```

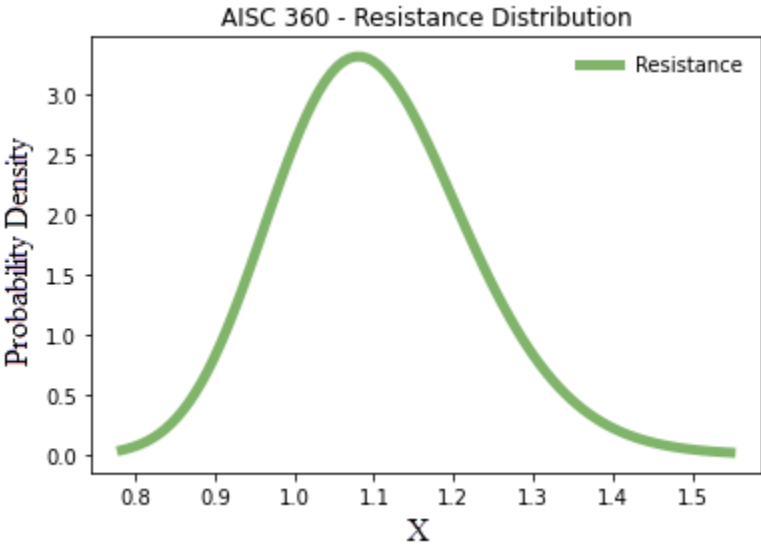


Figure 15 – AISC Resistance Bias Frequency Distribution Curve

3.5.2. Dead Load

The dead load is characterized by a normal probability distribution, with a mean of 1.05 and a COV of 0.1. The normal distribution curve is identical to the CSA S16 curve used in Section 3.4.2.

3.5.3. Live Load

The maximum live load during the life of the structure is characterized by a Gumbel probability distribution, with a mean of 1.0 and a COV of 0.25 [7]. For live load, the influence area affects the value of the parameters to be used. In this thesis, we have chosen values which correspond to an assumed influence area of $\sim 100\text{m}^2$ ($\sim 1000\text{ft}^2$) which is typical for steel structures.

The gumbel distribution curve can be generated using the `gumbel_r` function from Python's SciPy library. To produce a Gumbel distribution with a bias = 1.0 and COV = 0.25, a location factor of 0.889, and a scale factor of 0.196 must be used in the `gumbel_r` function. The distribution curve is shown in Figure 16.

x

```
= numpy.linspace(gumbel_r.ppf(0.001, loc, scale), gumbel_r.ppf(0.999, loc, scale), 100)
```

```
matplotlib.pyplot.plot(x, gumbel_r.pdf(x, loc, scale))
```

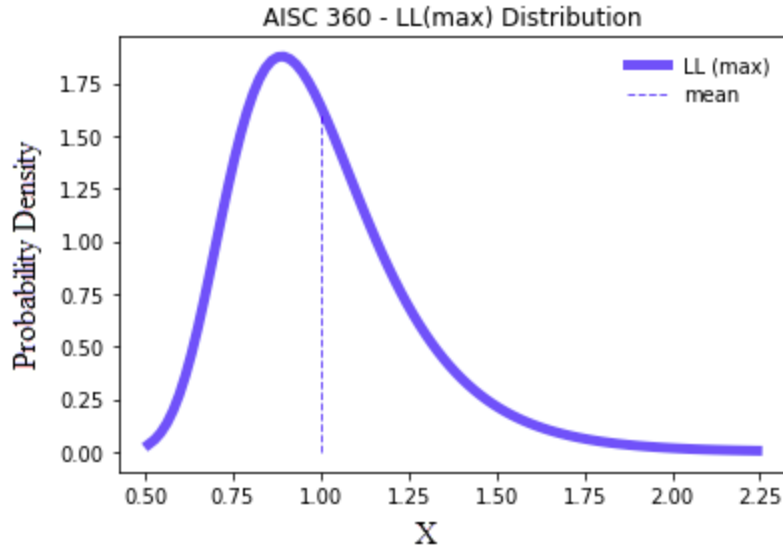


Figure 16 – AISC Live Load Bias Frequency Distribution Curve

The arbitrary point in time live load is characterized by a Gamma probability distribution, with a mean of 0.24 and a COV of 0.5. The distribution curve can be generated using the gamma function from Python’s SciPy library. To produce a Gamma distribution with a bias = 0.24 and COV = 0.5, a shape factor of 3.99, location factor of 0, and a scale factor of 0.0602 must be used in the gamma function. The distribution curve is shown in Figure 11.

x

`= numpy.linspace(gamma.ppf(0.001, a, loc, scale), gamma.ppf(0.999, a, loc, scale), 100)`

`matplotlib.pyplot.plot(x, weibull_min.pdf(x, s, loc, scale))`

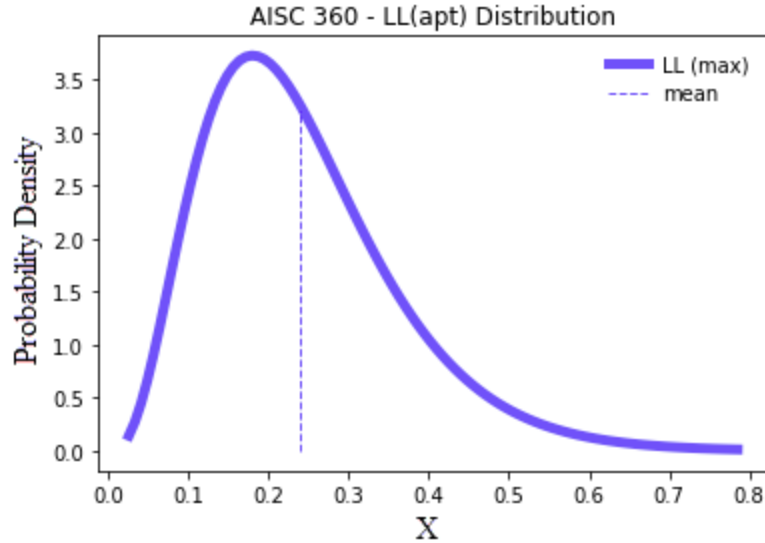


Figure 17 – AISC Live Load (Apt) Bias Frequency Distribution Curve

3.5.4. Wind Load

Wind load data used in reliability analysis in AISC is based on data from seven sites which give a broad geographical representation [7]. It was determined by Ellingwood et al that this data could be fitted very well to a Gumbel distribution [7]. The data was then used to compute the extreme values (u) and shape (α) of the distribution as $u_{max} = 0.65$, $\alpha_{max} = 4.45$, $u_{apt} = -0.021$, and $\alpha_{apt} = 18.7$.

From these values, the bias factor and coefficient of variation can be computed for both the maximum and arbitrary point in time cases using the following formulas as per the work of Benjamin and Cornell [17]:

$$mean = u + \frac{0.577}{\alpha} \quad (3-6)$$

$$std = \frac{\pi}{\sqrt{6} * \alpha} \quad (3-7)$$

$$cov = \frac{std}{mean} \quad (3-8)$$

Using these formula's, the statistical parameters for calculating wind load distribution functions can be solved for giving a mean of 0.78 and a COV of 0.37. The distribution curve can be generated using the `gumbel_r` function from Python's SciPy library. To produce a Gumbel distribution with a bias = 0.78 and COV = 0.37, a location factor of 0.65, and a scale factor of 0.225 must be used in the `gumbel_r` function. The distribution curve is shown in Figure 18.

x

`= numpy.linspace(gumbel_r.ppf(0.001, loc, scale), gumbel_r.ppf(0.999, loc, scale), 100)`

`matplotlib.pyplot.plot(x, gumbel_r.pdf(x, loc, scale))`

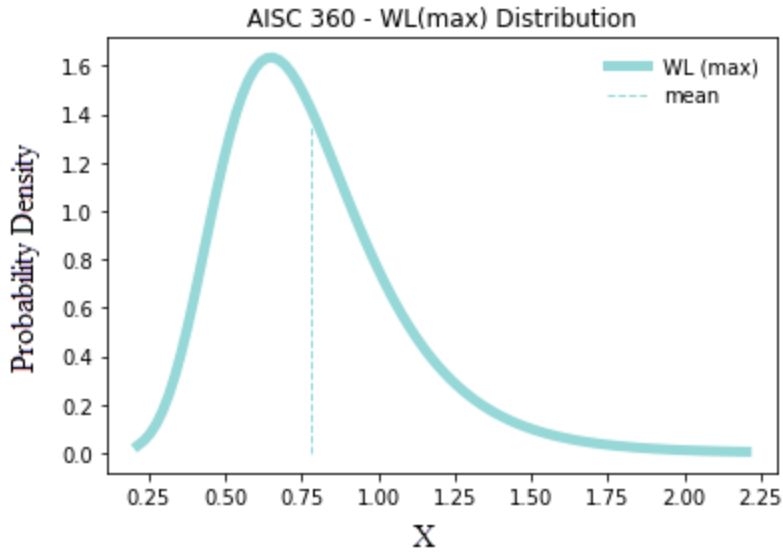


Figure 18 – CSA Wind Load (Max) Bias Frequency Distribution Curve

The arbitrary point in time wind load is characterized by a Gumbel probability distribution, with a mean of 0.01 and a COV of 0.069. The distribution curve can be generated using the `gumbel_r` function from Python’s SciPy library. To produce a Gumbel distribution with a bias = 0.01 and COV = 0.069, a location factor of 0.01, and a scale factor of 0.00056 must be used in the `gumbel_r` function. The distribution curve is shown in Figure 19.

x

```
= numpy.linspace(gumbel_r.ppf(0.001, loc, scale), gumbel_r.ppf(0.999, loc, scale), 100)
```

```
matplotlib.pyplot.plot(x, gumbel_r.pdf(x, loc, scale))
```

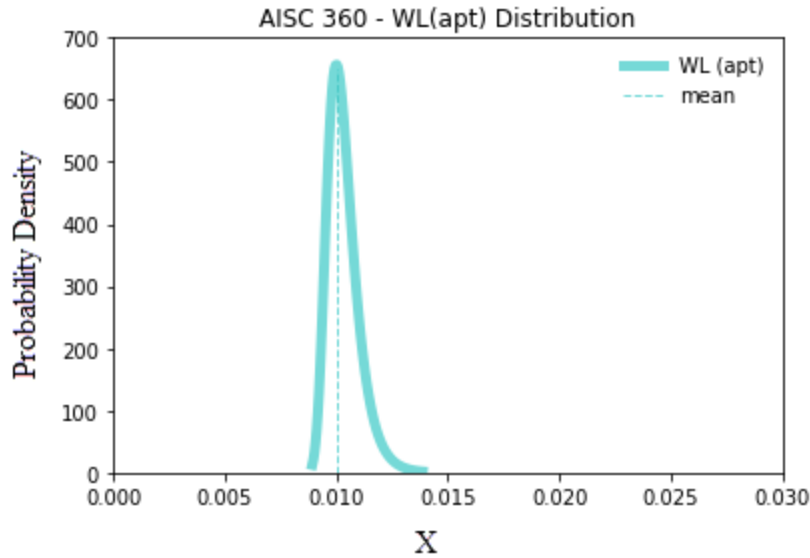


Figure 19 – CSA Wind Load (Apt) Bias Frequency Distribution Curve

3.5.5. Snow Load

Snow load data used in reliability analysis in AISC is based on data from water-equivalent loads at some 180 first order weather stations and snow depths at some 9000 additional sites which are then converted to loads through density-depth relations [7].

The maximum snow load during the life of the structure is characterized by a Lognormal probability distribution, with a mean of 0.82 and a COV of 0.26 [7]. The lognormal distribution curve can be generated using the lognorm function from Python’s SciPy library. To produce a Lognormal distribution with a bias = 0.82 and COV = 0.26, a shape factor = 0.21, location factor of -0.2, and a scale factor of 1.0 must be used in the lognorm function. The distribution curve is shown in Figure 20.

x

$= \text{numpy.linspace}(\text{gumbel_r.ppf}(0.001, \text{loc}, \text{scale}), \text{gumbel_r.ppf}(0.999, \text{loc}, \text{scale}), 100)$

```
matplotlib.pyplot.plot(x, gumbel_r.pdf(x, loc, scale))
```

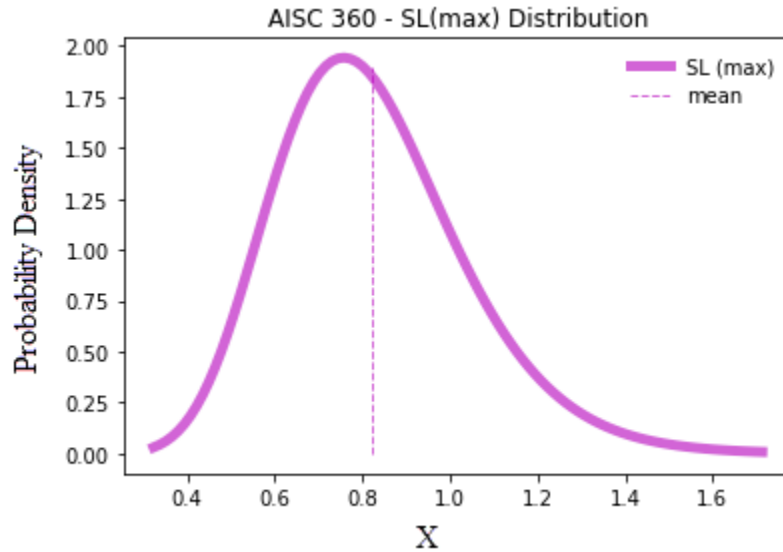


Figure 20 – CSA Snow Load (Max) Bias Frequency Distribution Curve

The arbitrary point in time wind load is characterized by a Lognormal probability distribution, with a mean of 0.2 and a COV of 0.73 [7]. The distribution curve can be generated using the lognorm function from Python’s SciPy library. To produce a Lognormal distribution with a bias = 0.2 and COV = 0.73, a shape factor = 0.144, location factor of -0.81, and a scale factor of 1.0 must be used in the lognorm function. The distribution curve is shown in Figure 21.

x

```
= numpy.linspace(gumbel_r.ppf(0.001, loc, scale), gumbel_r.ppf(0.999, loc, scale), 100)
```

```
matplotlib.pyplot.plot(x, gumbel_r.pdf(x, loc, scale))
```

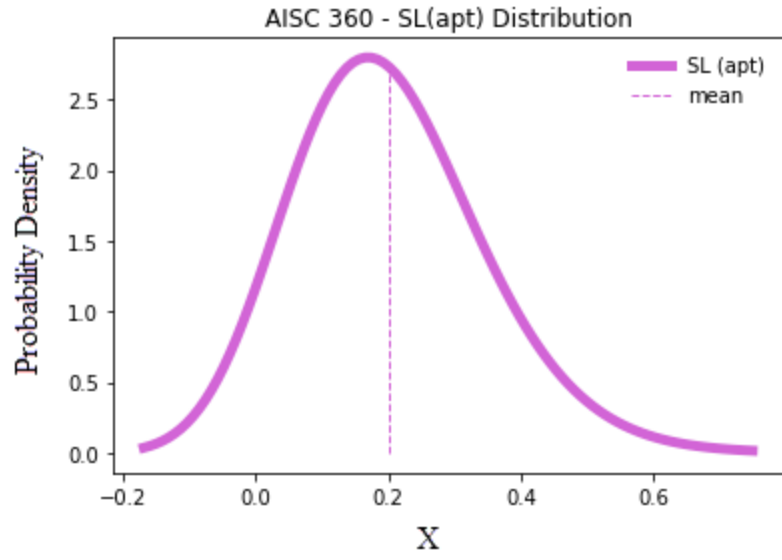


Figure 21 – AISC Snow Load (Apt) Bias Frequency Distribution Curve

Chapter 4. Reliability Analysis

4.1. Monte Carlo Simulation

4.1.1. General

In this thesis, the reliability index is computed using the Monte Carlo Simulation (MCS) method with consideration of the statistical distributions of the resistance and load variables, determined here, or obtained from the available literature. The basic concept of this method is to generate many tests quickly and randomly without having to do any physical experiment. To do so, a random value is generated for each design variable based on the probability distribution of that variable, and the random values of all the variables are then used to determine the safety margin. The process is repeated for many simulated variables. The reliability index is then computed by dividing the mean value of all the simulated safety margins by the corresponding standard deviation. The MCS method can also be used to compute the probability of failure by dividing the number of simulations of the safety margin bearing a negative sign by the total number of simulations. This approach is very robust and can be applied to almost any limit state formulation. The disadvantages of a MCS are that it is computationally inefficient. Many variables bounded to different constraints can require a lot of time and a lot of computations to approximate a solution. Also input parameters must be realistic and accurate. If poor parameters and constraints are input into the model, then poor results will be given as outputs.

The software used for this purpose is Python 3.9.7, Numpy 1.19.3, Scipy 1.5.4, and Matplotlib 3.3.3. Custom code has been written using these software packages to perform the MCS, using 500,000 iterations for each MCS. The Python software language is used to write the main code, the Scipy package is used for its probability distribution functions, the Numpy package is used for

its mathematical functions, and the Matplotlib package is used to plot results. A sample of the code is included in Appendix A, and a description of the theory behind the code with an example is detailed in Section 4.1.2.

4.1.2. CSA S16

For the MCS, the factored load combinations used by CSA-S16 must be considered, which are based on the NBCC [18]. The load combinations are shown in Table 3. The relationship between the reliability index and applied loads depends on the fraction of D, L, W, and S within the load combinations specified by the code.

Load Combination	Factored Load Combination
1	1.4D
2	1.25D + 1.5L + 1.0S
3	1.25D + 1.5L + 0.4W
4	1.25D + 1.5S + 1.0L
5	1.25D + 1.5S + 0.4W
6	1.25D + 1.4W + 0.5L
7	1.25D + 1.4W + 0.5S

Table 3 – Factored Load Combinations

For each combination, different ratios of L/D, W/D, and S/D are considered to produce reliability index curves. These can then be compared to the target reliability index. Since it is highly unlikely that the various loads will reach their peak values at the same time, a practical approach is needed when combining the loads on the structure. In this study, the total load effect is determined using Turkstra’s rule [19]. This approach assumes that the critical value of a combination of several loads is reached when one load takes on its maximum value while the remaining other loads are at their

arbitrary-point-in-time values. This produces the following four combinations since the dead load is assumed not to vary with time.

$$D + L_{max} + W_{apt}$$

$$D + L_{apt} + W_{max}$$

$$D + L_{max} + S_{apt}$$

$$D + L_{apt} + S_{max}$$

When combined with Table 3, this produces 13 load combinations to be examined, as shown in Table 4.

Load Combination	Factored Load Combination
1	1.4D
2	1.25D + 1.5L _{max} + 1.0S _{apt}
3	1.25D + 1.5L _{apt} + 1.0S _{max}
4	1.25D + 1.5L _{max} + 0.4W _{apt}
5	1.25D + 1.5L _{apt} + 0.4W _{max}
6	1.25D + 1.5S _{max} + 1.0L _{apt}
7	1.25D + 1.5S _{apt} + 1.0L _{max}
8	1.25D + 1.5S _{max} + 0.4W _{apt}
9	1.25D + 1.5S _{apt} + 0.4W _{max}
10	1.25D + 1.4W _{max} + 0.5L _{apt}
11	1.25D + 1.4W _{apt} + 0.5L _{max}
12	1.25D + 1.4W _{max} + 0.5S _{apt}

13	$1.25D + 1.4W_{apt} + 0.5S_{max}$
----	-----------------------------------

Table 4 - Factored Load Combinations using Turkstra's Rule

Where

L_{max} = Maximum Live Load

L_{apt} = Arbitrary Point in Time Live Load

W_{max} = Maximum Wind Load

W_{apt} = Arbitrary Point in Time Wind Load

S_{max} = Maximum Snow Load

S_{apt} = Arbitrary Point in Time Snow Load

4.1.2.1. Dead + Live

The case of dead load and live load is considered first. Values for the nominal dead and live loads are selected. This AISC 360 LRFD code was calibrated with the ASD code at $L/D = 3.0$, so that is the first case examined here, although a range of L/D ratios will be investigated. Using $DL = 200$ kN and $LL = 600$ kN, we then determine the critical factored load to be equal to 1150 kN ($1.25D = 250$ kN) + ($1.5L = 900$ kN). This gives required nominal strength of $R_n = 1278$ kN since the resistance factor in CSA for steel is 0.90.

$$Res = \frac{1.25 * 250kN + 1.5 * 600kN}{0.9} = 1278kN \quad (4-1)$$

Using the appropriate distribution functions for each load as discussed in Section 3.4, many random values can be generated for the resistance and loads. We set $n = 500,000$ simulations and use the appropriate bias factors and COV's determined in Section 3.4 to generate random values for each simulation.

$n = 500,000$

$Res_{dist} = \text{scipy.stats.lognorm.rvs}(s, loc, scale, n)$

$DL_{dist} = \text{scipy.stats.norm.rvs}(loc, scale, n)$

$LL_{dist} = \text{scipy.stats.gumbel_r.rvs}(loc, scale, n)$

Using these distributions of random values, we can determine the frequency distributions of R and Q, as follows.

$$R = Res_{dist} * Res \quad (4-2)$$

$$Q = DL_{dist} * DL + LL_{dist} * LL \quad (4-3)$$

Curves can be fitted to both sets of random values of R and Q, which can then be graphed as show in Figure 22. This gives the familiar load effect and resistance curves discussed previously and shown in Figure 6. The overlap in the curves represents the simulations where failure occurred.

Using python's numpy library, the mean and coefficient of variation can be determined for both R and Q. The reliability index can then be determined from the following formula [2]:

$$\beta = \frac{\ln(R_m/Q_m)}{\sqrt{V_R^2 + V_Q^2}} = 3.10 \quad (4-4)$$

$R_m = \text{mean value of the resistance, } R$

$Q_m = \text{mean value of the load effect, } Q$

$V_R = \text{coefficient of varitaion of the resistance, } R$

$V_Q = \text{coefficient of variation of the load effect, } Q$

The reliability index for this case is 3.10. The frequency distributions after running 50,000 simulations for a ratio of $L/D = 3.0$ is shown in Figure 22. A probability of failure can be determined by counting the number of simulations where $Q > R$. In this case there were 927 failures, which corresponds to a failure probability of 0.19%.

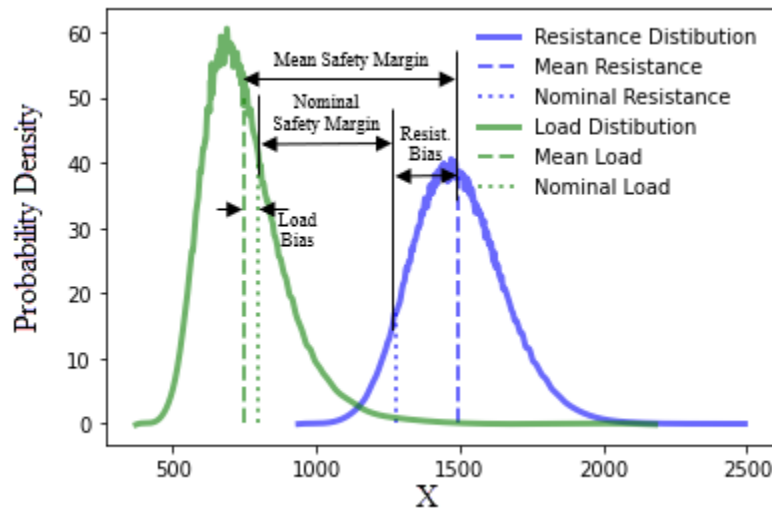


Figure 22 – Frequency Distributions For Random Values of Q and R with $L/D = 3.0$

We can repeat this process for different ratios of L/D , and we end up with the curve shown in Figure 23. CSA S16 and the NBCC specify a target reliability of $\beta_T=3.0$ as per [5], which is also indicated on the curve. Note the curve dips sharply at first since the Dead Load factor is decreased from 1.4 to 1.25 as soon as Live Load is present (L/D ratio > 0) before rising again and then flattening out approaching a value slightly below the target reliability of 3.

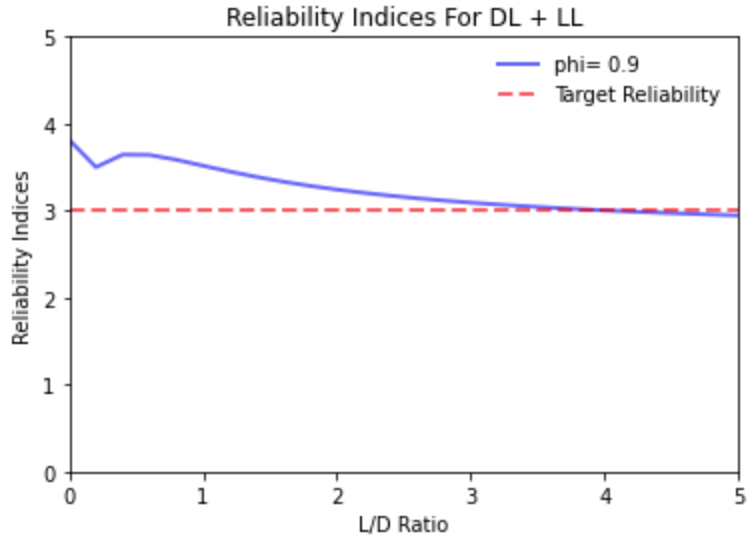


Figure 23 – CSA Reliability Indices for DL + LL and $\phi=0.9$

This curve can then be adjusted up and down by using different material factor values. This can be seen in Figure 24.

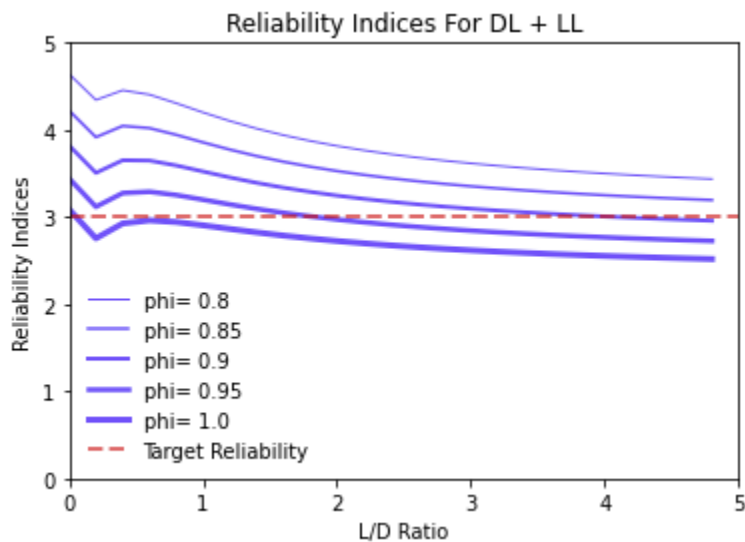


Figure 24 - CSA Reliability Indices for DL + LL and varying ϕ

4.1.2.2. Dead + Live + Wind

Looking next at D + L + W, we must consider cases 4,5,10, and 11 from Table 4. Running MCS's for each produces the following graphs for the case of $W/D = 0.25$ and varying L/D.

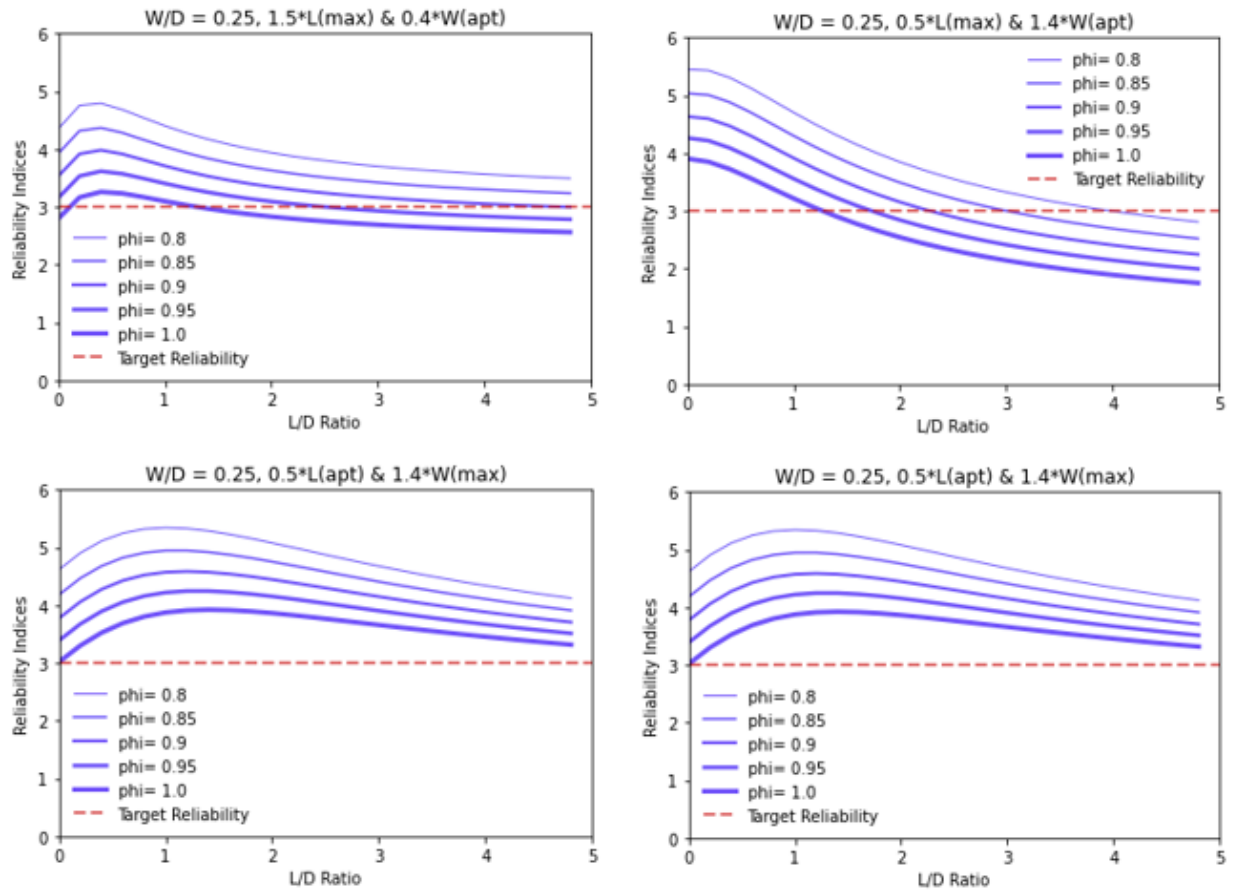


Figure 25 – CSA Reliability Indices for DL + LL + WL

We can combine these graphs into a single graph by taking the lowest reliability index value out of all four for each value of L/D ratio. This produces the graph shown in Figure 26. Looking at different ratios of W/D in the same manner produces the graphs shown in Figure 27 through Figure 29.

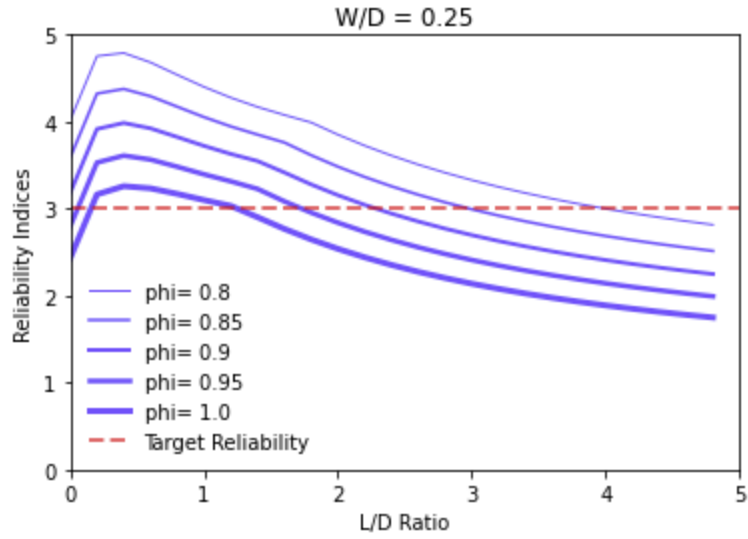


Figure 26 – CSA Reliability Indices for DL + LL + WL with W/D = 0.25

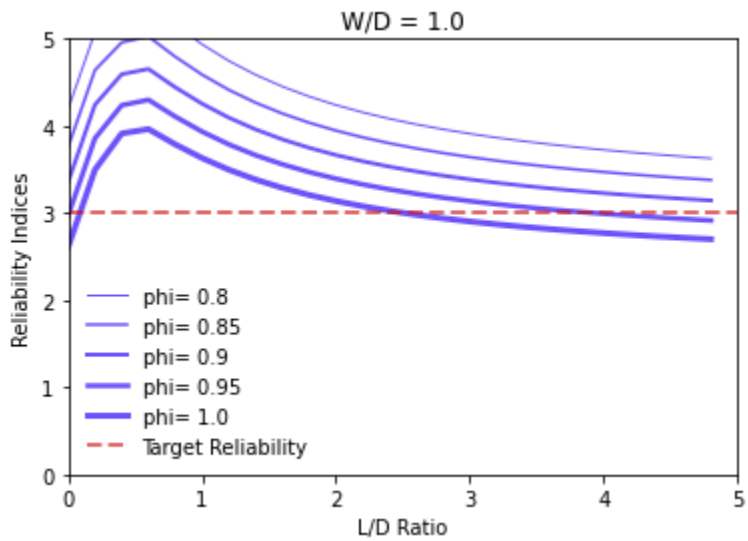


Figure 27 – CSA Reliability Indices for DL + LL + WL with W/D = 1.0

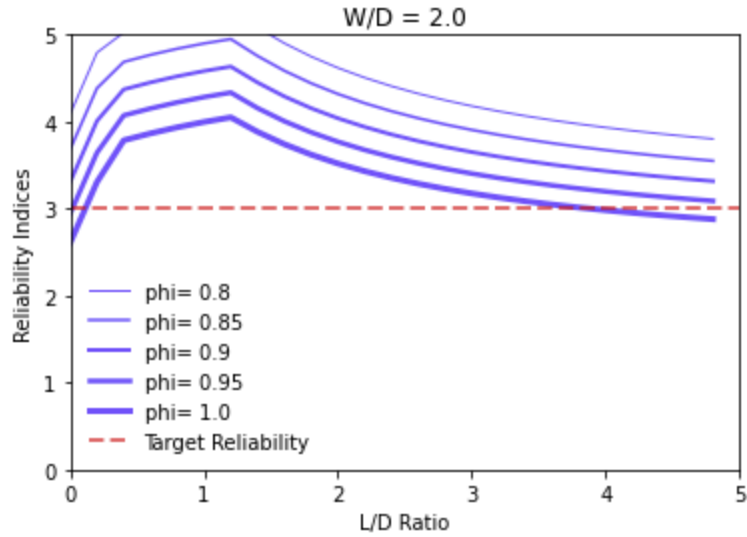


Figure 28 – CSA Reliability Indices for DL + LL + WL with W/D = 2.0

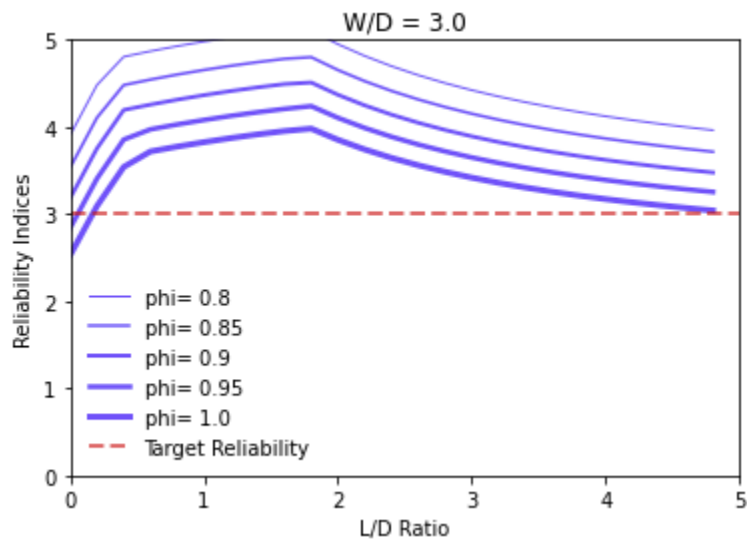


Figure 29 – CSA Reliability Indices for DL + LL + WL with W/D = 3.0

4.1.2.3. Dead + Live + Snow

For the scenario of D + L + S, we must consider cases 2, 3, 6, and 7 from Table 4. Running MCS's for each produces the following graphs for the case of S/D = 0.25 and varying S/D.

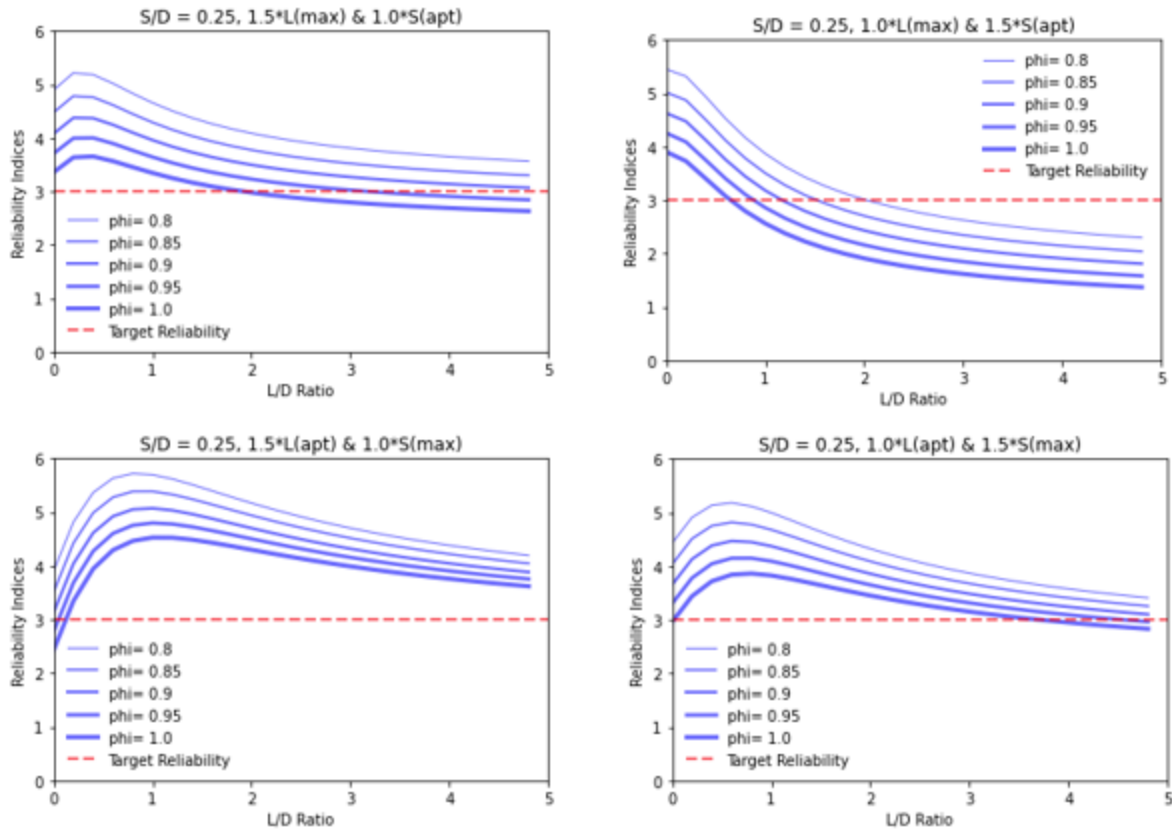


Figure 30 – CSA Reliability Indices for DL + LL + SL

We can combine these graphs into a single graph by taking the lowest reliability index value out of all four for each value of L/D ratio. This produces the graph shown in Figure 31. Looking at different ratios of W/D in the same manner produces the graphs shown in Figure 27 through Figure 29.

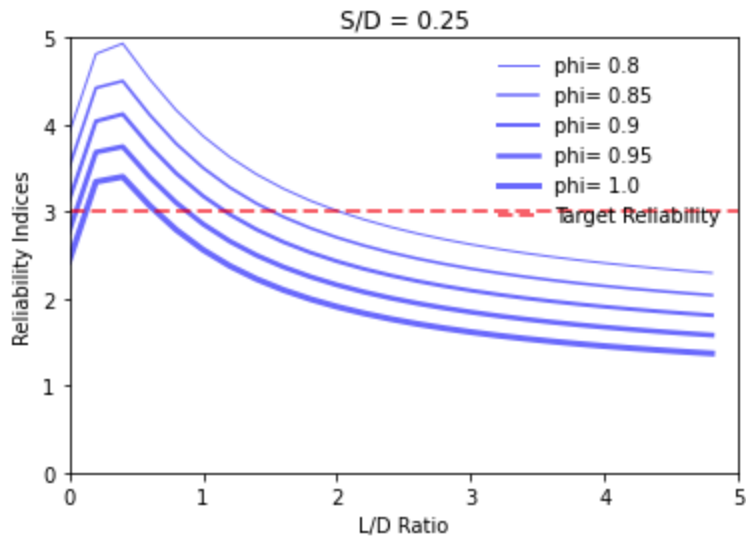


Figure 31 – CSA Reliability Indices for DL + LL + SL with S/D = 0.25

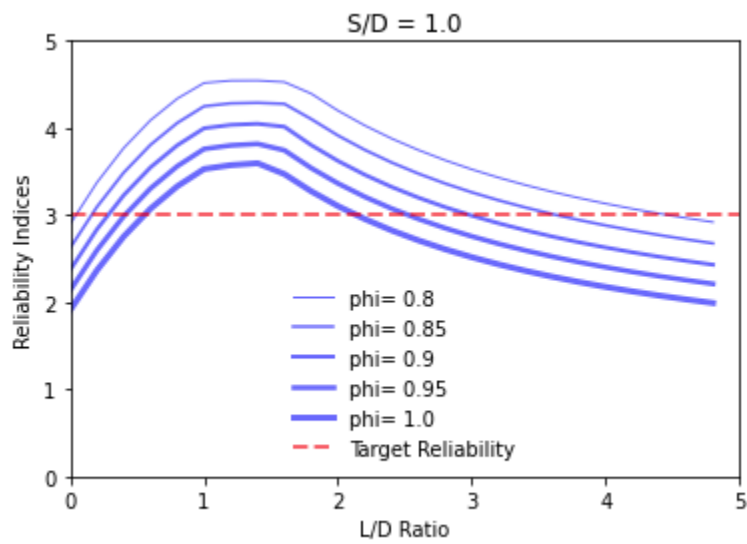


Figure 32 – CSA Reliability Indices for DL + LL + SL with S/D = 1.0

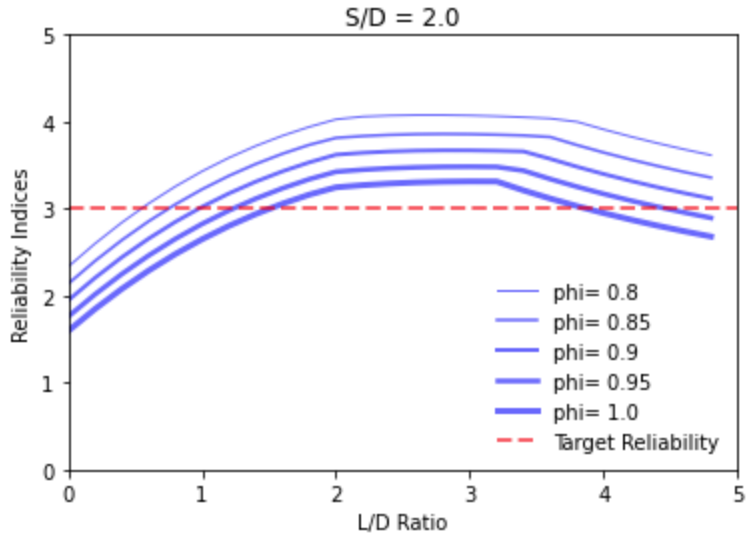


Figure 33 – CSA Reliability Indices for DL + LL + SL with S/D = 2.0

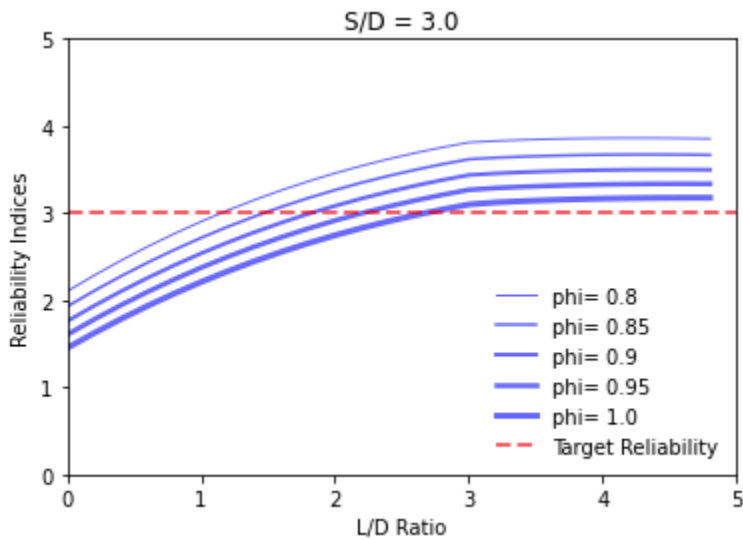


Figure 34 – CSA Reliability Indices for DL + LL + SL with S/D = 3.0

4.1.3. AISC 360

The same exercise is performed for the factored load combinations used by AISC 360, which are based on ASCE/SEI 7 [9]. The load combinations are shown in Table 5. The relationship between the reliability index and applied loads depends on the fraction of D, L, W, and S within the load combinations specified by the code.

Load Combination	Factored Load Combination
1	1.4D
2	1.2D + 1.6L + 0.5S
3	1.2D + 1.0L + 1.0W + 0.5S
4	1.2D + 1.6S + 0.5W
5	1.2D + 1.6S + 0.5L

Table 5 – Factored Load Combinations

For each combination, different ratios of L/D, W/D, and S/D are considered to produce reliability index curves. These can then be compared to the target reliability index.

The cases of D, L, W, and S can be represented by the maximum effect of three combinations since the dead load is assumed not to vary with time. We can again use Turkstra’s rule [19] in combination with Table 5 to produce the 10 load combinations shown in Table 6.

Load Combination	Factored Load Combination
1	1.4D
2	1.2D + 1.6L _{max} + 0.5S _{apt}
3	1.2D + 1.6L _{apt} + 0.5S _{max}
4	1.2D + 1.0L _{max} + 1.0W _{apt} + 0.5S _{apt}
5	1.2D + 1.0L _{apt} + 1.0W _{max} + 0.5S _{apt}
6	1.2D + 1.0L _{apt} + 1.0W _{apt} + 0.5S _{max}
7	1.2D + 1.6S _{max} + 0.5W _{apt}
8	1.2D + 1.6S _{apt} + 0.5W _{max}
9	1.2D + 1.6S _{apt} + 0.5L _{max}

10	$1.2D + 1.6S_{\text{apt}} + 0.5L_{\text{max}}$
----	--

Table 6 – Factored Load Combinations using Turkstra’s Rule

Where

L_{max} = Maximum Live Load

L_{apt} = Arbitrary Point in Time Live Load

W_{max} = Maximum Wind Load

W_{apt} = Arbitrary Point in Time Wind Load

S_{max} = Maximum Snow Load

S_{apt} = Arbitrary Point in Time Snow Load

4.1.3.1. Dead + Live

The MCS to determine AISC reliability indices is carried out in the same manner as was done for CSA in Section 4.1.2.

The first scenario we can compare is that of L + D only. The same nominal dead and live loads are selected ($D = 200 \text{ kN}$ and $L = 600 \text{ kN}$), giving a L/D ratio of 3.0. We then determine the critical factored load to be equal to 1200 kN ($1.2D = 240\text{kN}$) + ($1.6L = 960\text{kN}$). We then find the required nominal strength to be $R_n \approx 1333 \text{ kN}$ since the resistance factor in AISC for steel is 0.90.

$$DL = 200kN$$

$$LL = 600kN$$

$$Res = \frac{1.2 * 200kN + 1.6 * 600kN}{0.9} = 1333kN \quad (4-5)$$

$$\beta = \frac{\ln(R_m/Q_m)}{\sqrt{V_R^2 + V_Q^2}} = 2.73 \quad (4-6)$$

Using the same process as Section 4.1.2, as well as Equation (4-6), the reliability index is determined to be 2.73. The frequency distributions for AISC after running 50000 simulations for a ratio of $L/D = 3.0$ is shown in Figure 35. There were 2337 failures which gives a probability of failure of 0.47%. It can be seen the overlap between the curves is slightly larger than in the case of CSA.

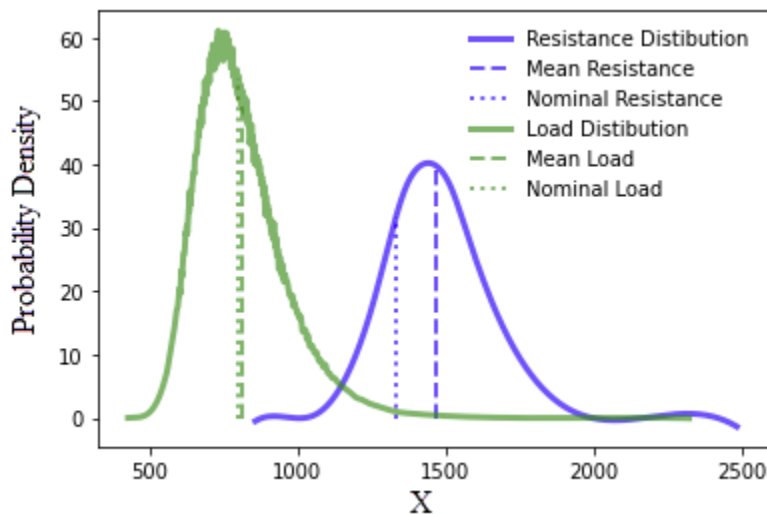


Figure 35 – Frequency Distributions For Random Values of Q and R with $L/D = 3$

The reliability index for AISC with $L/D = 3.0$ is slightly lower than the value for CSA with $L/D = 3.0$. This is expected since AISC 360 specifies a target reliability of 2.6 for $L/D = 3.0$.

We can repeat this process for different ratios of L/D , and we end up with the curve shown in Figure 23. The AISC target reliability is also indicated on the curve.

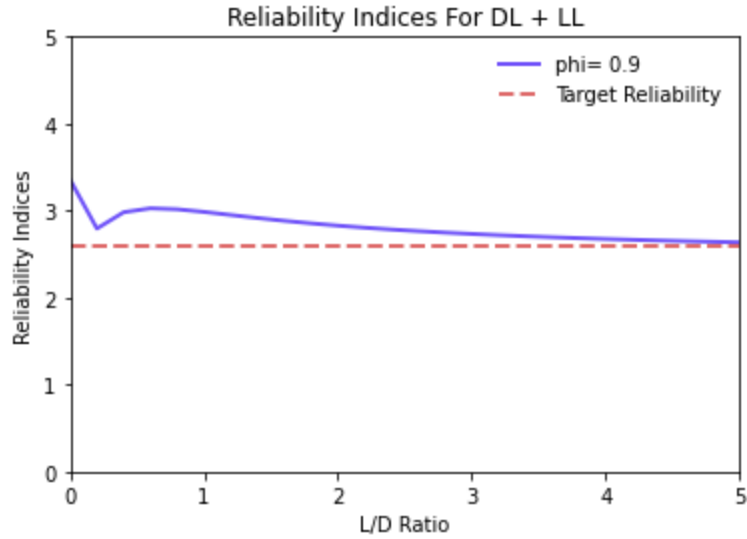


Figure 36 – AISC Reliability Indices for DL + LL and $\phi=0.9$

This curve can then be adjusted up and down by using different material factor values. This can be seen in Figure 37.

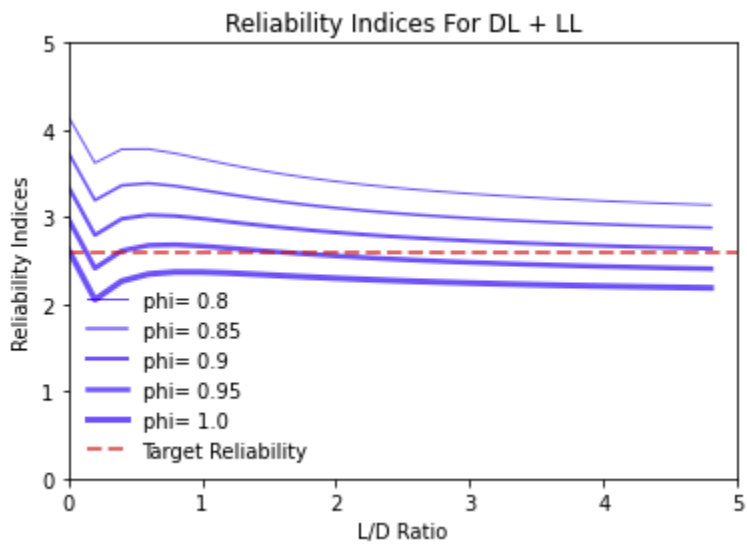


Figure 37 – AISC Reliability Indices for LL + DL and Varying ϕ

4.1.3.2. Dead + Live + Wind

Looking first at D + L + W with S = 0, we must consider cases 4, 5, and 6 from Table 6. Running MCS's for each case and using the lowest reliability index from all combined produces graphs for varying cases of W/D with varying L/D.

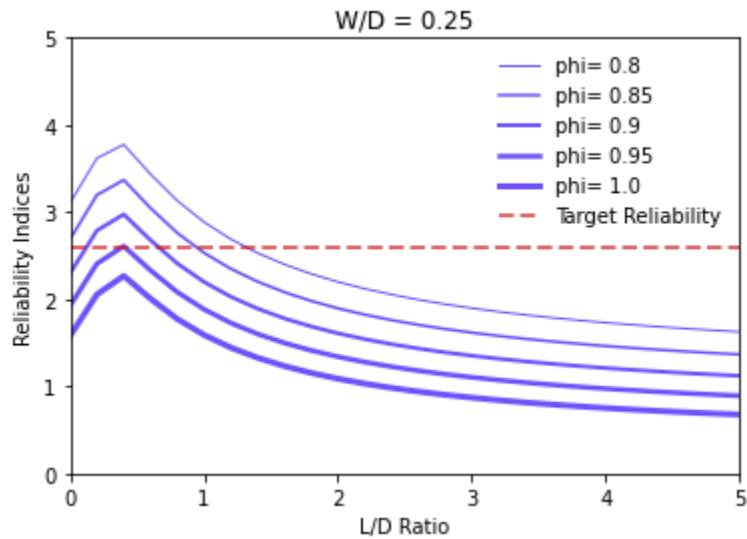


Figure 38 – AISC Reliability Indices for DL + LL + WL with W/D = 0.25

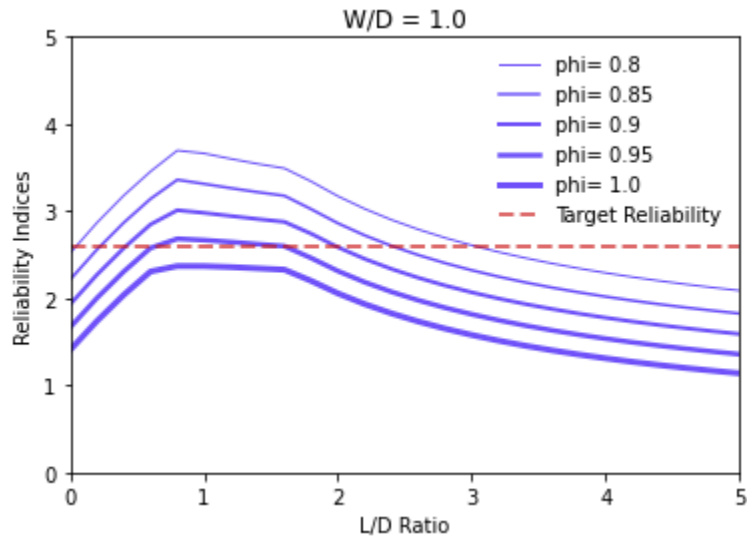


Figure 39 – AISC Reliability Indices for DL + LL + WL with W/D = 1.0

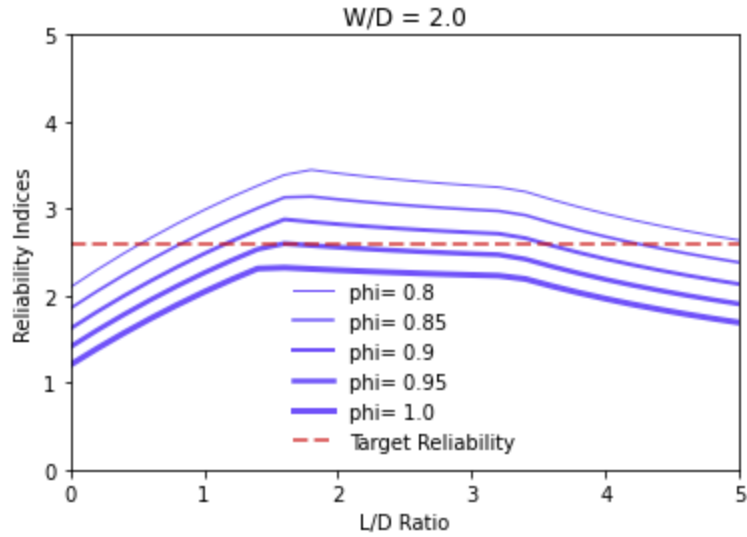


Figure 40 – AISC Reliability Indices for DL + LL + WL with W/D = 2.0

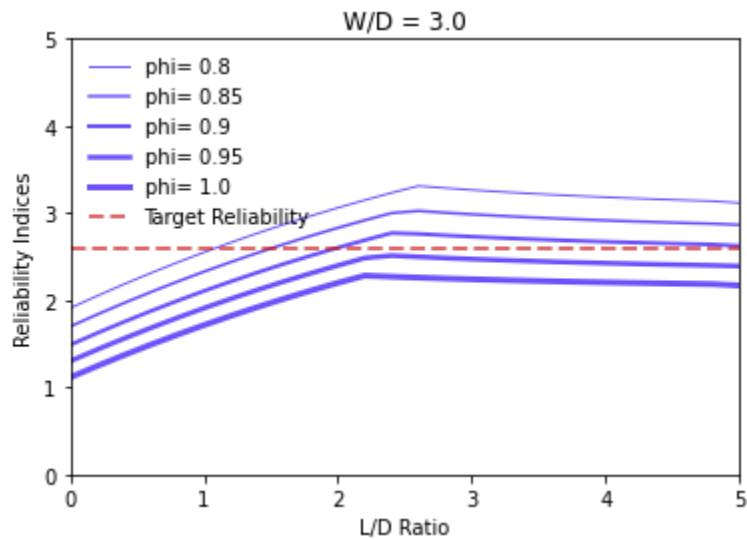


Figure 41 – AISC Reliability Indices for DL + LL + WL with W/D = 2.0

4.1.3.3. Dead + Live + Snow

For the scenario of D + L + S, we must consider cases 2, 3, 9, and 10 from Table 6. Running MCS's for each case and using the lowest reliability index from all combined produces graphs for varying cases of S/D with varying L/D.

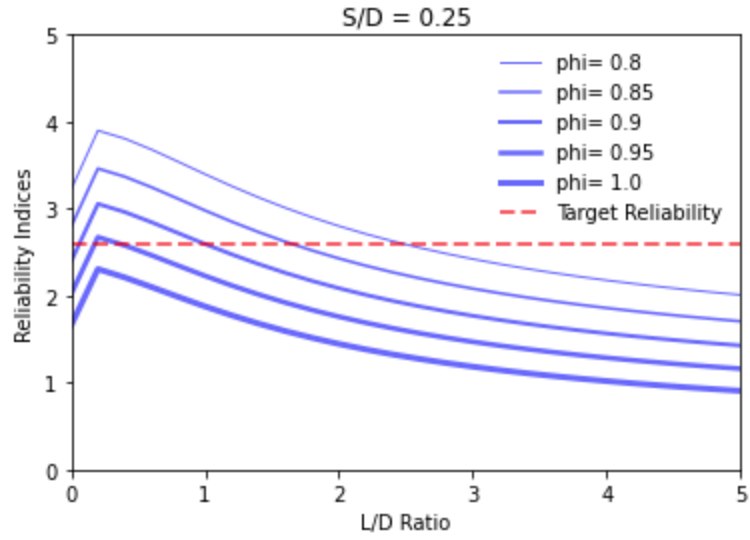


Figure 42 – AISC Reliability Indices for DL + LL + SL with $S/D = 0.25$

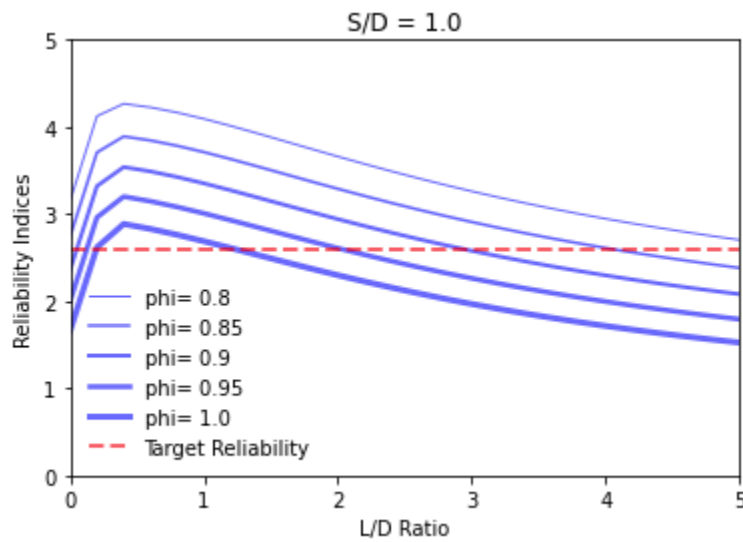


Figure 43 – AISC Reliability Indices for DL + LL + SL with $S/D = 1.0$

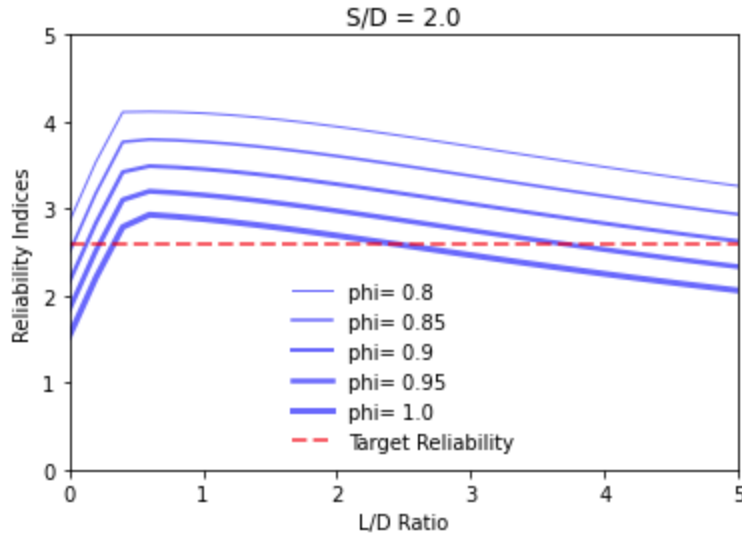


Figure 44 – AISC Reliability Indices for DL + LL + SL with S/D = 2.0

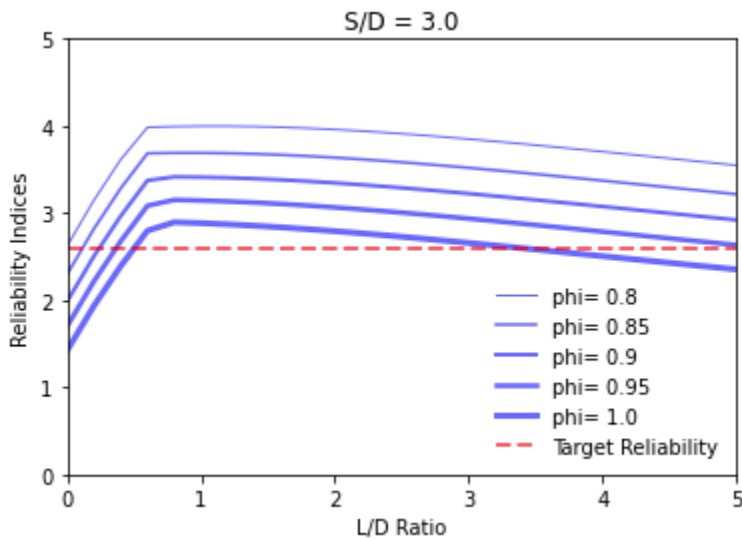


Figure 45 – AISC Reliability Indices for DL + LL + SL with S/D = 3.0

4.1.4. Target Reliabilities

Results and target reliability graphs from the above sections agree well with the literature review and assumed target reliabilities of the AISC 360 Specification and the CSA S16 Standard. This is easiest to see in the case of dead load plus live load in sections 4.1.2.1 and 4.1.3.1. In each case the MCS produces reliability index graphs where the curve rises slightly for low ratios of L/D, and

then approaches the target reliability as the L/D ratio increases. This validates the MCS method used and allows it to be proposed to calibrate strength formulas from other codes for use in the CSA S16 standard.

For the purposes of this study, the L+D case will be used to calibrate proposed strength formulas to a target reliability of 3.0 for use in the CSA S16 standard.

Chapter 5. Reliability-Based Strength Formula Development

5.1. Reliability-Based Strength Formula Model

Considering the reliability indices are different between CSA and AISC, we cannot simply adopt the AISC torsional strength formulas into the CSA standard. However, an approach can be developed to adopt equations between the codes while maintaining the appropriate reliability index. The process is detailed in a flowchart in Figure 46. It is proposed that the desired strength formula can be adopted into the CSA S16 standard as follows:

1. Choose a proposed strength formula for adoption into the CSA S16 standard, through experiment, testing, or adoption from another code.
2. Find experimental data to compare/verify the proposed formula against.
3. Use the ratio of experimental to predicted strength to determine the Bias and COV of the Professional (P) factor.

$$Bias_p = mean\left(\frac{R_{exp}}{R_{pred}}\right) \quad (5-1)$$

$$COV_p = \frac{std\left(\frac{R_{exp}}{R_{pred}}\right)}{mean\left(\frac{R_{exp}}{R_{pred}}\right)} \quad (5-2)$$

4. Use the Bias and COV for Material (M) and Fabrication (F) factors from a reference such as Ref [20].
5. Combine the Bias and COV values from PMF to get an overall Bias and COV for R_n and use them to generate a lognormal distribution function (R_{ndist}).

6. Using the geometric properties of one of the test specimens from Step 2, calculate the nominal resistance using the proposed strength formula from Step 1.
7. Starting with D+L, and a ratio of L/D = 3.0, solve for the Live Load and the Dead Load using Equation (3-1) by substituting in the Resistance from Step 6, the appropriate LL and DL factors (1.5 and 1.25 respectively), and the L/D ratio.

$$DL = \frac{\phi R_n}{(1.25 + (3.0 * 1.5))} \quad (5-3)$$

$$LL = \frac{\phi R_n}{\left(\left(\frac{1.25}{3.0}\right) + 1.5\right)} \quad (5-4)$$

8. Using the appropriate distribution functions for each load as discussed in Section 3.4, as well as the distribution function from Step 5, generate a statistically significant amount of random values of R, and Q, using Equation (4-2) and Equation (4-3).

$$R = R_{ndist} * R_n \quad (5-5)$$

$$Q = DL_{dist} * DL + LL_{dist} * LL \quad (5-6)$$

9. Calculate the reliability index of the proposed strength formula using Equation (4-4).

$$\beta = \frac{\ln(R_m/Q_m)}{\sqrt{V_R^2 + V_Q^2}} \quad (5-7)$$

10. Repeat steps 7 through 9 over a range of L/D ratios and generate a reliability index curve.
11. Compare the reliability index curve from Step 10 to the curve shown in Figure 23. If the reliability indices are similar, the proposed formula can be proposed to be adopted by the CSA S16 standard.
12. If the reliability index is too low or too high (not within 5% of target reliability) , adjust the strength formula, recalculate the Bias and COV from Step 3, and repeat the process until the desired reliability curve is found in Step 11.

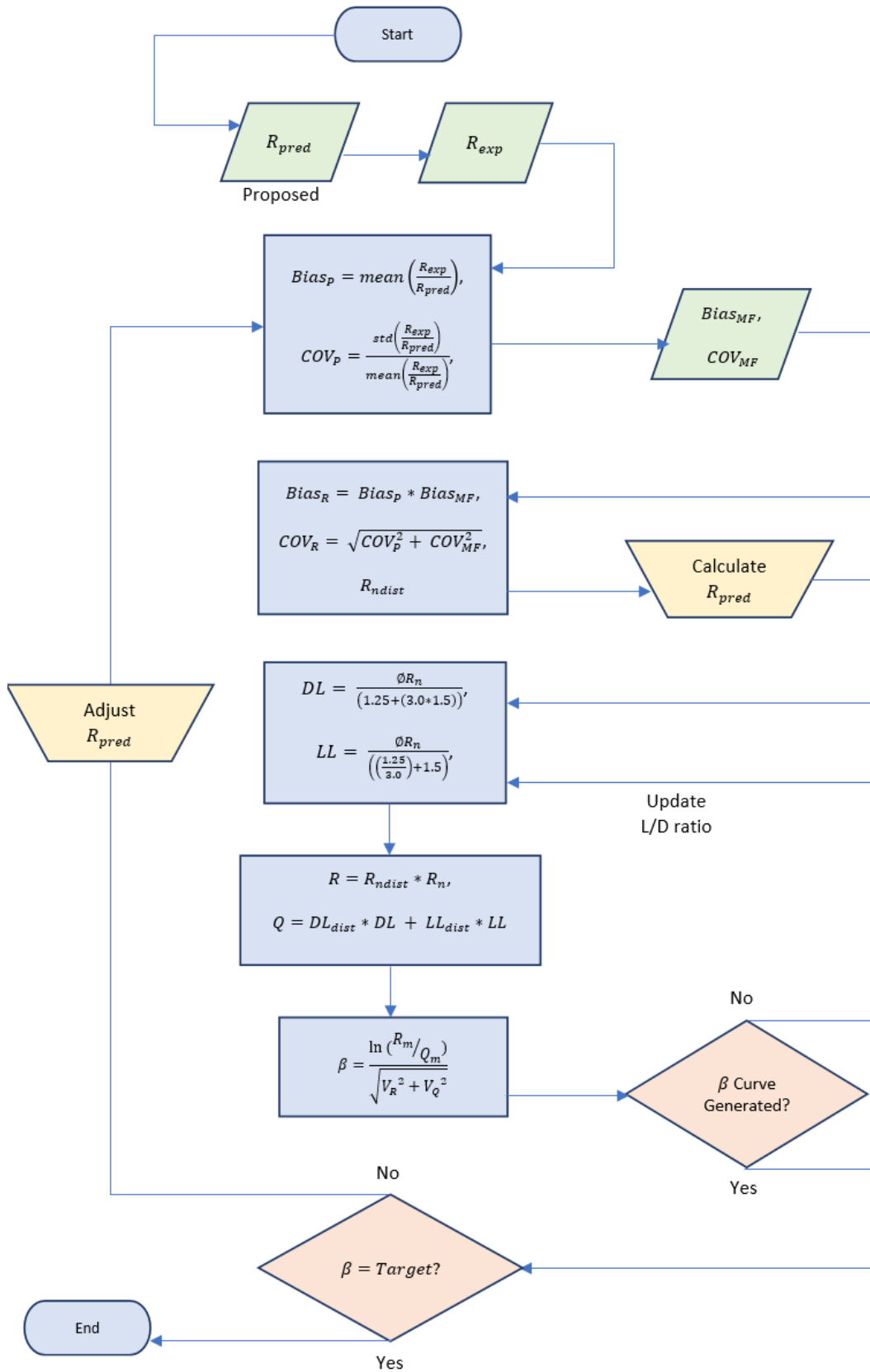


Figure 46 – Reliability-Based Strength Formula Model

This model will be used to develop torsional strength formulas for inclusion in the CSA S16 Standard in the following sections.

5.2. Torsional Strength of Round HSS

In developing a round HSS torsional strength formula for inclusion in the CSA S16 standard, we will use the AISC formula as a starting point in our proposed model. The strength equation for round HSS sections given by AISC 360 is as follows:

$$R_n = F_{cr}C \quad (5-8)$$

Where:

$C = \text{HSS Torsional Constant}$

and F_{cr} shall be the larger of:

$$F_{cr} = \frac{1.23E}{\sqrt{\frac{L}{D} \left(\frac{D}{T}\right)^{\frac{5}{4}}}} \quad (5-9)$$

and:

$$F_{cr} = \frac{0.60E}{\left(\frac{D}{t}\right)^{\frac{3}{2}}} \quad (5-10)$$

and shall not exceed:

$$F_{cr} = 0.6F_y \quad (5-11)$$

The model modifies this formula with consideration of natural variations in material properties, fabrication tolerances and deviation of the model from experimental outcomes, that is:

$$R = R_n * (PMF) \quad (5-12)$$

Where:

R_n = the nominal resistance value

P = Professional Factor – Accounts for ratio of tested capacity to theoretical

M = Material Factor – Accounts for ratio of actual to nominal material properties

F = Fabrication/Geometric Factor – Accounts for ratio of actual to nominal material thicknesses

The professional factor must be based on experimental data. For the case of Round HSS sections, experimental data for torsional resistance can be found in Torsional Strengthening of Steel Circular Hollow Sections (CHS) using CFRP composites, Ref [21]. This paper is mostly concerned with resistance of carbon fibre reinforced polymer round HSS sections, however, the data for the control group of standard non-reinforced round HSS sections can be used for the purpose of this study.

Specimen ID	Experimental Torsional Capacity, R_{exp} (kN*m)	Predicted Torsional Capacity, R_n (kN*m)	R_{exp}/R_n	Failure Mode
CHS1-1	8.74	8.44	1.04	Yielding
CHS1-2	8.71	8.44	1.03	Yielding
CHS2-1	9.80	8.46	1.16	Yielding
CHS2-2	9.92	8.46	1.17	Yielding
CHS3-1	14.60	13.27	1.10	Yielding
CHS3-2	14.26	13.27	1.07	Yielding
CHS4-1	16.64	13.70	1.21	Yielding
CHS4-2	N/A	13.70	N/A	Welding Failure

CHS5-1	26.36	21.35	1.23	Yielding
CHS5-2	N/A	21.35	N/A	Welding Failure

Table 7 – Round HSS Experimental Data

The bias and the coefficient of variation of the professional factor must be estimated from the distribution of the ratio of R_{exp}/R_n , in which R_n is the nominal torsional strength given by Equation (5-8) and R_{exp} is the actual strength from the experiment. Based on the ratio R_{exp}/R_n from the data of the 10 tests in Table 7 the bias factor and the coefficient of variation of the professional factor are then estimated as: Bias = 1.128 and COV = 0.065.

Next, the combined effect of the factors M and F, denoted by MF, is considered. A common bias factor and a common coefficient of variation MF based on the material and geometric properties of Round HSS sections can be found in Review of resistance factor for steel: Data collection, Ref [20] and taken as: Bias = 1.35 and COV = 0.097.

Since both P and MF obey the lognormal distribution, then the product follows strictly the lognormal distribution, and the bias factor and the coefficient of variation of the torsional resistance of Round HSS sections can be computed as:

$$Bias = \bar{P} * \overline{MF} = 1.523 \quad (5-13)$$

and:

$$COV = \sqrt{V_P^2 + V_{MF}^2} = 0.117 \quad (5-14)$$

Which produces the distribution shown in Figure 47.

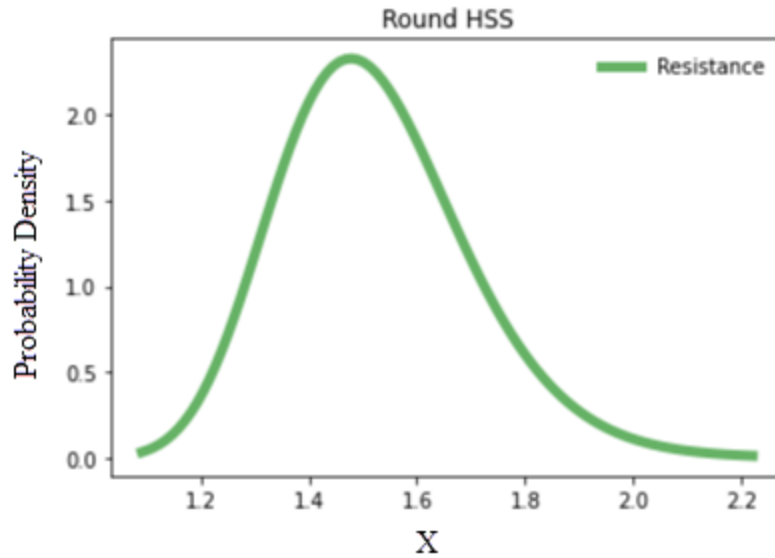


Figure 47 – Frequency Distribution Curve of Round HSS using AISC strength formula

These values can now be used to verify the reliability index were the AISC formula for torsional strength of Round HSS sections be used with the CSA S16 standard. To do this, the steps in Section 4.1.2 can be followed using the statistical parameters for Resistance determined above in place of those stated in Table 1. This produces the reliability index graph shown in Figure 48.

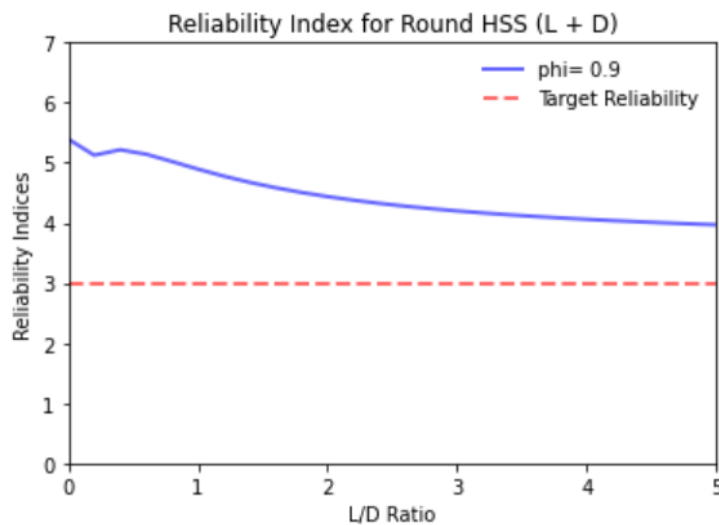


Figure 48 – Reliability Index Graph for Round HSS using AISC strength formula

Using the strength formula from AISC unaltered gives a reliability index which approaches 4.0, well above the CSA target.

To adjust the reliability index curve closer to the target, we can propose a new equation closer to the equation for shear strength of Round HSS sections used by CSA S16, which corresponds to a 10% increase. To do this we can use the following updated equations in place of F_{CR} in Equation (5-8).

F_{cr} shall be the larger of:

$$F_{cr} = 1.1 \frac{1.23E}{\sqrt{\frac{L}{D} \left(\frac{D}{T}\right)^{\frac{5}{4}}}} \quad (5-15)$$

and:

$$F_{cr} = 1.1 \frac{0.60E}{\left(\frac{D}{t}\right)^{\frac{3}{2}}} \quad (5-16)$$

and shall not exceed:

$$F_{cr} = 1.1(0.6F_y) \quad (5-17)$$

A comparison of the torsional strength of Round HSS sections using the AISC equations and the proposed CSA equation is shown in Figure 49.

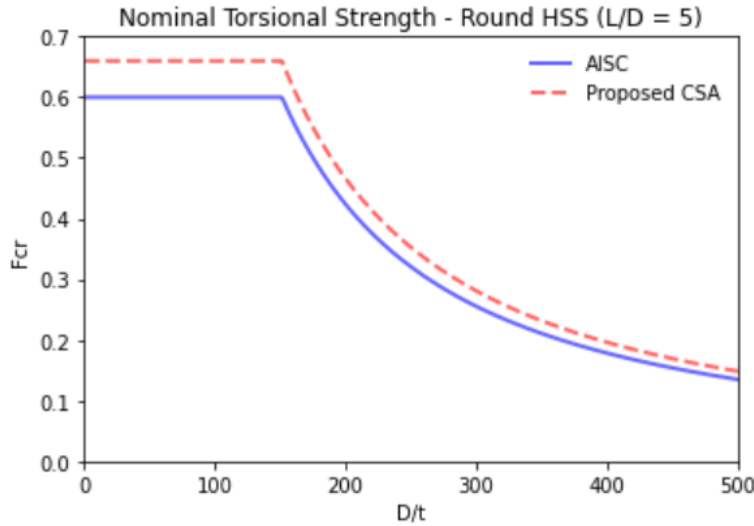


Figure 49 – Nominal Torsional Strength of Round HSS Members – AISC 360 and Proposed CSA S16

Using this formula produces the updated predicted strength values shown in Table 8.

Specimen ID	Experimental Torsional Capacity, R_{exp} (kN*m)	Predicted Torsional Capacity, R_n (kN*m)	R_{exp}/R_n	Failure Mode
CHS1-1	8.74	9.29	0.94	Yielding
CHS1-2	8.71	9.29	0.94	Yielding
CHS2-1	9.80	9.31	1.05	Yielding
CHS2-2	9.92	9.31	1.07	Yielding
CHS3-1	14.60	14.60	1.00	Yielding
CHS3-2	14.26	14.60	0.98	Yielding
CHS4-1	16.64	15.07	1.10	Yielding
CHS4-2	N/A	15.07	N/A	Welding Failure
CHS5-1	26.36	23.49	1.12	Yielding
CHS5-2	N/A	23.49	N/A	Welding Failure

Table 8 – Updated Round HSS Experimental Data

Using these new ratios of R_{exp}/R_n from the data of the 10 tests in Table 8 the new bias factor and the coefficient of variation of the professional factor are then estimated as: Bias = 1.025 and COV = 0.065.

These new factors are combined with the previously determined bias factor and coefficient of variation of MF to produce a bias factor = 1.384 and COV = 0.065 for the proposed torsional resistance of Round HSS sections.

These new values can be used to produce the reliability index graph shown in Figure 50.

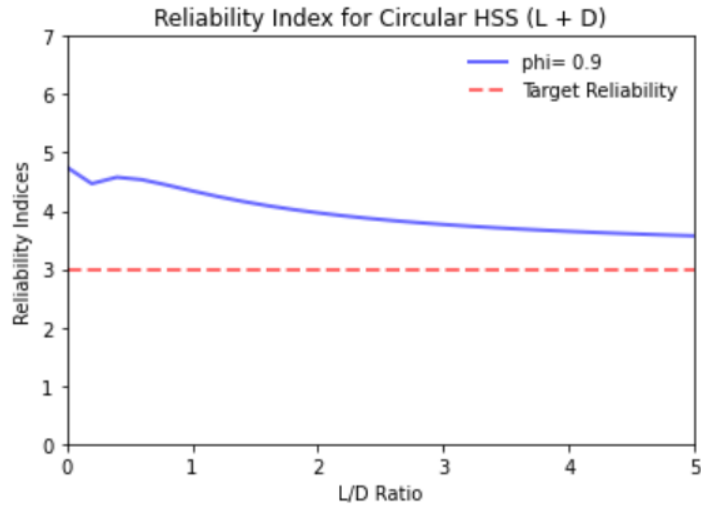


Figure 50 - Reliability Index Graph for Round HSS using Proposed CSA strength formula

Using the proposed CSA strength formula gives a reliability index which approaches 3.5. This is still above the target reliability of CSA. Through trial and error, it is determined that a 25% increase could be used on Equation (5-9), Equation (5-10), and Equation (5-11) to give the appropriate target reliability of 3.0 for the torsional strength of round HSS sections in CSA S16. However, Equation (5-15), Equation (5-16), and Equation (5-17) give better consistency with the shear strength equations of round HSS sections already in use in CSA S16. The recommendation is to use the following resistance factor when using the AISC 360 torsional strength formula for round HSS sections when designing to the CSA S16 standard:

$$\phi = 0.9 * 1.1 \approx 1.0 \quad (5-18)$$

5.3. Torsional Strength of Rectangular HSS

In developing a rectangular HSS section torsional strength formula for inclusion in the CSA S16 standard, we will use the AISC formula as a starting point in the proposed model. The strength equation for rectangular HSS sections given by AISC 360 is as follows:

$$R_n = F_{cr}C \quad (5-19)$$

Where:

$$C = \text{HSS Torsional Constant} = 2(B - t)(H - t)t - 4.5(4 - \pi)t^3$$

When $h/t \leq 2.45\sqrt{E/F_y}$:

$$F_{cr} = 0.6F_y \quad (5-20)$$

When $2.45\sqrt{E/F_y} < h/t \leq 3.07\sqrt{E/F_y}$:

$$F_{cr} = \frac{0.6F_y(2.45\sqrt{E/F_y})}{\left(\frac{h}{t}\right)} \quad (5-21)$$

When $3.07\sqrt{E/F_y} < h/t \leq 260$:

$$F_{cr} = \frac{0.458\pi^2 E}{\left(\frac{h}{t}\right)^2} \quad (5-22)$$

The model modifies this formula with consideration of natural variations in material properties, fabrication tolerances and deviation of the model from experimental outcomes, that is:

$$R = R_n * (PMF) \quad (5-23)$$

Where:

R_n = the nominal resistance value

P = Professional Factor – Accounts for ratio of tested capacity to theoretical

M = Material Factor – Accounts for ratio of actual to nominal material properties

F = Fabrication/Geometric Factor – Accounts for ratio of actual to nominal material thicknesses

The professional factor must be based on experimental data. For the case of rectangular HSS sections, experimental data for torsional resistance can be found in the work of Devi et al, Ridley-Ellis, and Marshall [22] [23] [24]. The first two studies are mostly concerned with torsional resistance of perforated rectangular HSS sections, however, the data for the control groups of standard non-perforated rectangular HSS sections can be used for the purpose of this study.

Specimen ID	Experimental Torsional Capacity, R_{exp} (kN*m)	Predicted Torsional Capacity, R_n (kN*m)	R_{exp}/R_n	Source
RHS1-1	5.36	5.07	1.06	[22]
RHS1-2	5.38	5.07	1.06	[22]
TT4	43.1	57.99	0.74	[23]
TT3	38.8	51.22	0.76	[23]
TT7	53.2	64.14	0.83	[23]
TT14	53.6	64.14	0.84	[23]
TT8	49.6	62.94	0.79	[23]
A	2.78	3.72	0.75	[24]
B	4.56	6.12	0.74	[24]

C	9.36	12.81	0.73	[24]
D	15.9	21.20	0.75	[24]
E	11.6	14.32	0.81	[24]
F	8.35	12.45	0.67	[24]
G	2.78	3.66	0.76	[24]
H	3.54	4.19	0.85	[24]
I	4.56	5.66	0.81	[24]

Table 9 – Rectangular HSS Experimental Data

The bias and the coefficient of variation of the professional factor must be estimated from the distribution of the ratio of R_{exp}/R_n , in which R_n is the nominal torsional strength given by Equation (5-19) and R_{exp} is the actual strength from the experiment. Based on the ratio R_{exp}/R_n from the data of the 16 tests in Table 9 the bias factor and the coefficient of variation of the professional factor are then estimated as: Bias = 0.81 and COV = 0.13.

Next, the combined effect of the factors M and F, denoted by MF, is considered. A common bias factor and a common coefficient of variation MF based on the material and geometric properties of rectangular HSS sections can be found in Ref [20] and taken as: Bias = 1.35 and COV = 0.097.

Since both P and MF obey the lognormal distribution, then the product follows strictly the lognormal distribution, and the bias factor and the coefficient of variation of the torsional resistance of rectangular HSS sections can be computed as:

$$Bias = \bar{P} * \overline{MF} = 1.09 \quad (5-24)$$

and:

$$COV = \sqrt{V_P^2 + V_{MF}^2} = 0.16 \quad (5-25)$$

Which produces the distribution shown in Figure 51.

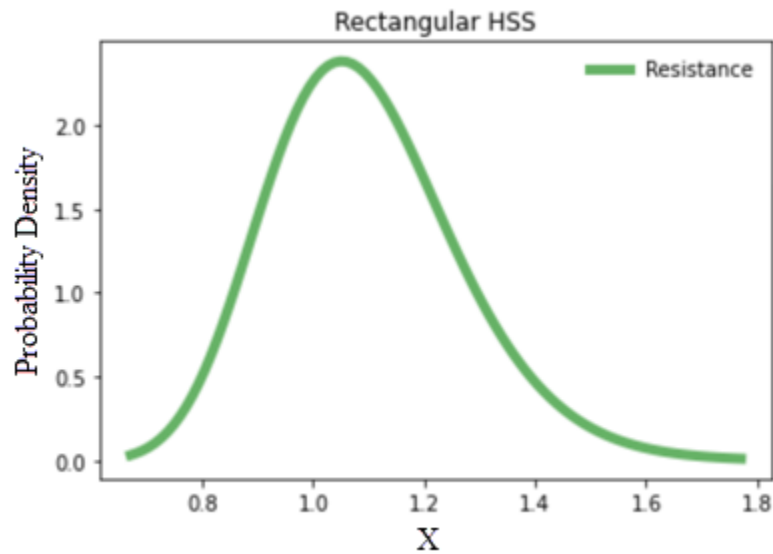


Figure 51 – Frequency Distribution Curve of Rectangular HSS using AISC strength formula

These values can now be used to verify the reliability index were the AISC formula for torsional strength of rectangular HSS sections be used with the CSA S16 standard. To do this, the steps in Section 4.1.3 can be followed using the statistical parameters for Resistance determined above in place of those stated in Table 1. This produces the reliability index graph shown in

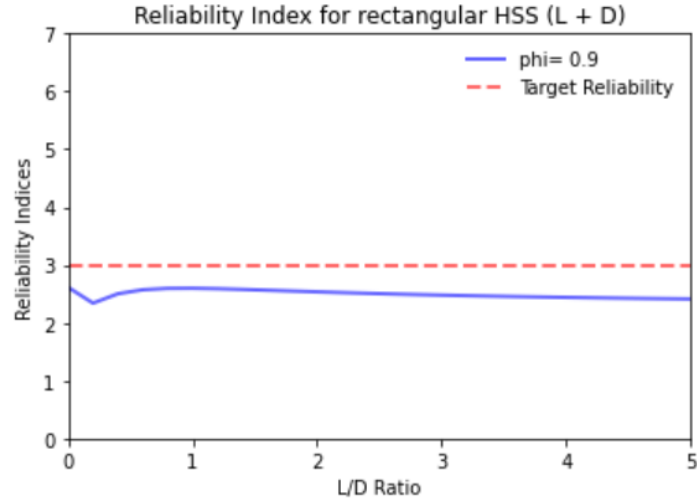


Figure 52 – Reliability Index Graph for Rectangular HSS using AISC strength formula

Using the strength formula from AISC unaltered gives a reliability index which approaches 2.5, below the CSA target.

To adjust the reliability index curve closer to the target, we can propose a new equation. Through trial and error as per the proposed model, the following updated equations are proposed to be used in place of F_{CR} in Equation (5-19), which corresponds to a 17% reduction in strength:

When $h/t \leq 2.45\sqrt{E/F_y}$:

$$F_{cr} = 0.83(0.6F_y) \tag{5-26}$$

When $2.45\sqrt{E/F_y} < h/t \leq 3.07\sqrt{E/F_y}$:

$$F_{cr} = 0.83 \frac{0.6F_y(2.45\sqrt{E/F_y})}{\left(\frac{h}{t}\right)} \tag{5-27}$$

When $3.07\sqrt{E/F_y} < h/t \leq 260$:

$$F_{cr} = 0.83 \frac{0.458\pi^2 E}{\left(\frac{h}{t}\right)^2} \quad (5-28)$$

A comparison of the torsional strength of rectangular HSS sections using the AISC equations and the proposed CSA equation is shown in Figure 53.

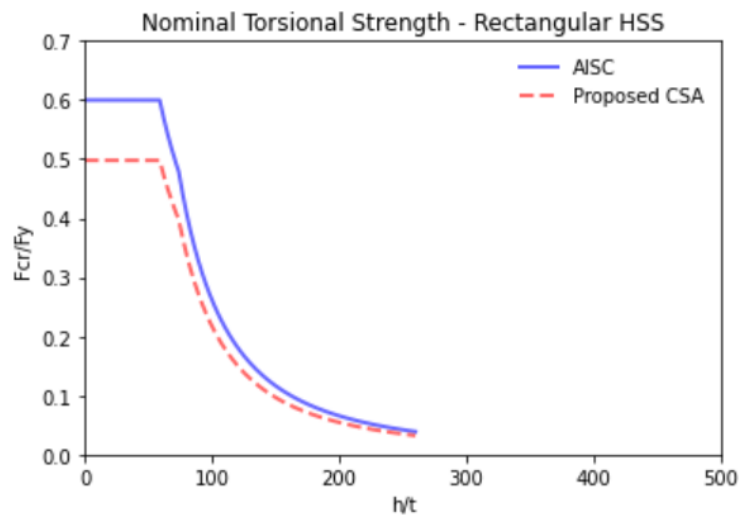


Figure 53 – Nominal Torsional Strength of Rectangular HSS Members – AISC 360 and Proposed CSA S16

Using this formula produces the updated predicted strength values shown in Table 10.

Specimen ID	Experimental Torsional Capacity, R_{exp} (kN*m)	Predicted Torsional Capacity, R_n (kN*m)	R_{exp}/R_n	Source
RHS1-1	5.36	4.21	1.27	[22]
RHS1-2	5.38	4.21	1.28	[22]
TT4	43.1	48.13	0.90	[23]
TT3	38.8	42.51	0.91	[23]
TT7	53.2	53.24	1.00	[23]
TT14	53.6	53.24	1.00	[23]
TT8	49.6	52.24	0.95	[23]
A	2.78	3.09	0.90	[24]

B	4.56	5.08	0.90	[24]
C	9.36	10.63	0.88	[24]
D	15.9	17.60	0.90	[24]
E	11.6	11.89	0.98	[24]
F	8.35	10.33	0.81	[24]
G	2.78	3.04	0.92	[24]
H	3.54	3.48	1.02	[24]
I	4.56	4.69	0.97	[24]

Table 10 – Updated Rectangular HSS Experimental Data

Using these new ratios of R_{exp}/R_n from the data of the 16 tests in Table 10 the new bias factor and the coefficient of variation of the professional factor are then estimated as: Bias = 0.97 and COV = 0.13.

These new factors are combined with the previously determined bias factor and coefficient of variation of MF to produce a bias factor = 1.31 and COV = 0.16 for the proposed torsional resistance of rectangular HSS sections.

These new values can be used to produce the reliability index graph shown in Figure 54.

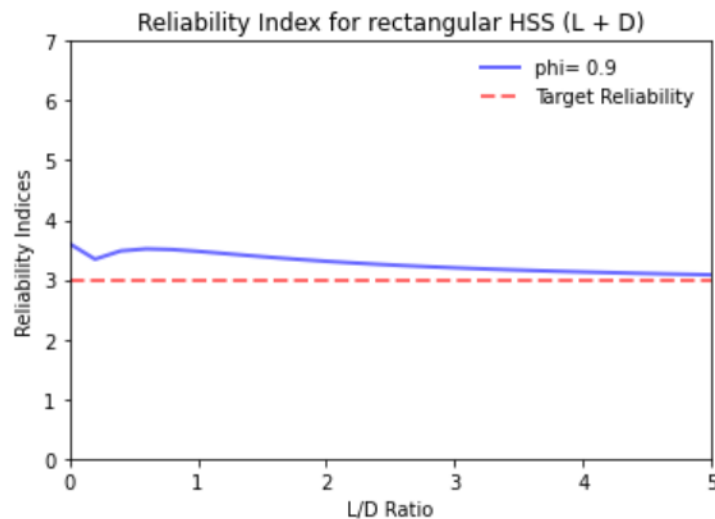


Figure 54 - Reliability Index Graph for Rectangular HSS using Proposed CSA strength formula

Using the proposed CSA strength formula gives a reliability index which approaches 3, which is in line with the target reliability of CSA S16.

It is unexpected to recommend a 17% reduction in AISC rectangular HSS section torsional strength, while recommending a 10% increase in AISC round HSS section torsional strength to meet desired target reliabilities for CSA S16. This is due to the test data used for rectangular HSS torsional strength not agreeing well with torsional theory. The test data is consistently 20% lower than the predicted strength. This is discussed in detail by Ridley-Ellis [23], and a reason for the anomalies is investigated, but not determined. In the absence of further test data, the recommendations given here will remain as is, but further testing is recommended. The recommendation is to use the following resistance factor when using the AISC 360 torsional strength formula for rectangular HSS sections when designing to the CSA S16 standard:

$$\phi = 0.9 * 0.83 = 0.75 \quad (5-29)$$

Chapter 6. Conclusion and Recommendations

6.1. General

A reliability-based approach for adopting strength formulas for use in CSA S16 Standard would benefit engineers by allowing more flexibility and options when designing steel structures.

To adopt the use of strength formulas from other sources for use in the CSA S16 standard, it is important to establish appropriate design guidelines and resistance factors to be used which will ensure the proper target reliability recommended by the CSA Standards Committee.

In this study, a series of reliability analyses were performed to verify the target reliabilities of both the CSA S16 Standard and the AISC 360 specification. This analysis was performed over a wide range of live-to-dead load ratios, L/D , wind-to-dead load ratios, W/D , and snow-to-dead load ratios, S/D . Results of this part of the thesis showed that the reliability graphs produced agreed well with the literature review and assumed target reliabilities of the AISC 360 Specification and the CSA S16 Standard. This validates the MCS method used and allows it to be proposed to calibrate strength formulas from other codes for use in the CSA S16 standard.

Then, an iterative reliability-based approach was proposed and used to calibrate proposed strength formulas in accordance with the desired target reliability of the CSA S16 standard. Strength formulas for both round HSS and rectangular HSS sections are proposed.

Analysis was performed using the Monte Carlo Simulation method and well-established probabilistic resistance and load models obtained from the available sources used by both standards.

The load models considered in this thesis included the dead, live, wind, and snow loads. Assuming a reference period of 50 years for building structures, the loads were combined following

Turkstra's rule. Reliability indices were examined and compared for varying ratios of L/D, W/D, and S/D. The reliability indices matched the target reliability indices of the code, and thus validated the MCS approach used.

6.2. Results and Discussion

Results of this investigation led to the following conclusions for adoption of AISC 360 clauses for use in the CSA S16 standard:

- The AISC 360 torsional strength formula for round HSS sections can be adopted into the CSA S16 standard with a resistance factor $\phi = 1.0$. This corresponds to a 10% increase in capacity from the AISC formula while still maintaining the desired target reliability for the CSA S16 standard.
- The AISC 360 torsional strength formula for rectangular HSS sections can be adopted into the CSA S16 standard with a resistance factor $\phi = 0.75$. This corresponds to a 17% reduction in capacity from the AISC formula while still maintaining the desired target reliability for the CSA S16 standard.

These recommendations for adopting the two torsional strength equations into the CSA S16 Standard don't completely align. However, they do fit well with the experimental data used, and make sense when taking into account the anomalies in in rectangular HSS torsional strength testing discussed by Ridley-Ellis, and Marshall [23] [24].

6.3. Future Work

Recommended future work is as follows:

- Verify the conclusions discussed here using FEA. A companion thesis to this one by Bartlett [25] examines the conclusions discussed here to consider the adoption of torsional strength calculations from the AISC 360 Specification for use in the CSA S16 Standard.
- Verify the conclusions discussed here over a wider variety of h/t and D/t ratios, as most test data available were within the lower ranges of h/t and D/t ratios and not at risk of local buckling.
- As discussed, it is unexpected to recommend a 17% reduction in AISC rectangular HSS section torsional strength, while recommending a 10% increase in AISC round HSS section torsional strength to meet desired target reliabilities for CSA S16. Further test data is needed to confirm these results, and to verify the anomalies in rectangular HSS torsional strength testing discussed in Ridley-Ellis, and Marshall [23] [24].
- Use the reliability-based model to verify the reliability index provided by the torsional strength equations for wide-flange sections proposed by Ashkinadze [13], or other similar sources.

References

- [1] CSA Group, CAN/CSA S16-19 - Design of Steel Structures, Toronto, Ontario, Canada: CSA Group, 2019.
- [2] American Institute of Steel Construction, ANSI/AISC 360-16 - Specification for Structural Steel Buildings, Chicago, Illinois, United States: American Institute of Steel Construction, 2016.
- [3] T. V. Galambos, "A Comparison of Canadian, Mexican, and United States Steel Design Standards," *AISC Engineering Journal*, 1999.
- [4] D. Allen, Limit States Design—A Probabilistic Study, *Canadian Journal of Civil Engineering*, 1975.
- [5] F. Bartlett, H. Hong and Z. W., "Load factor calibration for the proposed 2005 edition of the National Building Code of Canada: Statistics of loads and load effects," *Canadian Journal of Civil Engineering*, pp. 429-439, 2003.
- [6] F. Bartlett, H. Hong and W. Zhou, "Load factor calibration for the proposed 2005 edition of the National Building Code of Canada: Companion-action load combinations," *Canadian Journal of Civil Engineering*, pp. 440-448, 2003.

- [7] B. Ellingwood, T. V. Galambos, J. G. MacGregor and C. A. Cornell, "Development of a Probability Based Load Criterion for American National Standard A58," *Building Code Requirements for Minimum Design Loads in Buildings and Other Structures*, 1980.
- [8] A. N. S. Institute, "ANSI A58.1 Minimum Design Loads For Buildings And Other Structures," 1982.
- [9] A. S. o. C. Engineers, ASCE/SEI 7 - Minimum Design Loads and Associated Criteria for Buildings and Other Structures.
- [10] T. V. Galambos, "Load and Resistance Factor Design," *Engineering Journal - American Institute of Steel Construction*, 1980.
- [11] CAN/CSA S136-07 - North American specification for the design of cold-formed steel structural members, CSA Group, 2016.
- [12] M. Leblouba and S. Tabsh, "Reliability-based shear design of corrugated web steel beams for AISC 360 specification and CSA-S16 standard," *Engineering Structures*, vol. 215, 2020.
- [13] K. Ashkinadze, "Proposals for limit states torsional strength design of wide-flange steel members," *Canadian Journal of Civil Engineering*, vol. 35, pp. 200-209, 2008.
- [14] R. G. Driver and D. Kennedy, "Combined flexure and torsion of I-shaped steel beams," *Canadian Journal of Civil Engineering*, pp. 124-139, 1989.
- [15] Y.-L. Pi and N. S. Trahair, "Plastic-Collapse Analysis of Torsion," *Journal of Structural Engineering*, vol. 121, no. 10, 1995.

- [16] S. Timoshenko, "Theory of bending, torsion, and buckling of thin-walled members of open cross sections," 1953.
- [17] J. R. Benjamin and C. A. Cornell, Probability, Statistics, and Decision for Civil Engineers, Mineola, New York: DOVER PUBLICATIONS, INC, 1970.
- [18] N. R. C. o. Canada, National Building Code of Canada, 2015.
- [19] C. J. Turkstra, Theory of Structural Design Decisions, Waterloo, Ont: Solid Mechanics Division, University of Waterloo, 1970.
- [20] F. M. Bartlett and B. J. Schmidt, "Review of resistance factor for steel: Data collection," *Canadian Journal of Civil Engineering*, vol. 29, no. 1, pp. 98-108, 2011.
- [21] C. Wu, L. He, E. Ghafoori and X.-L. Zhao, "Torsional Strengthening of Steel Circular Hollow Sections (CHS) using CFRP composites," *Engineering Structures*, vol. 171, pp. 806-816, 2018.
- [22] S. V. Devi, T. G. Singh and K. D. Singh, "Cold-formed steel square hollow members with circular perforations subjected to torsion," *Journal of Constructional Steel Research*, 2019.
- [23] D. Ridley-Ellis, "Rectangular hollow sections with circular web openings: fundamental behaviour in torsion, bending and shear," *PhD thesis, University of Nottingham*, 2000.
- [24] J. Marshall, "Torsional behaviour of structural rectangular hollow sections," *The Structural Engineer*, vol. 49, no. 8, pp. 375-379, 1971.

[25] S. Bartlett, Finite Element Analysis Of Steel Sections In Torsion And Combined Torsion
Using Ansi/Aisc 360-16 For Adaptation In CAN/CSA S16-19, St. John's, 2020.

Appendix A – Monte Carlo Simulation Sample

The following code details the Monte Carlo Simulation used to produce the CSA reliability indices graph for DL + LL and $\phi=0.9$.

```

import numpy as np
from scipy.stats import norm
from scipy.stats import lognorm
from scipy.stats import gumbel_r
import matplotlib.pyplot as plt

mat= 0.9
LL_fact = 1.5
DL = 200
n=500000

Res_dist = lognorm.rvs(0.125, 0.1622, 1, n)
DL_dist = norm.rvs(1.05, 0.1, n)
LL_dist = gumbel_r.rvs(0.793, 0.188, n)

LL_ratio = 0

plot_x = []
plot_y = []

while(LL_ratio <= 5):
    LL = DL*LL_ratio
    if LL_ratio == 0:
        DL_fact = 1.4
    else:
        DL_fact = 1.25

    Res = ((DL*DL_fact)+(LL*LL_fact))/mat
    FOS = (Res_dist*Res)/(DL_dist*DL + LL_dist*LL)
    MOS = FOS-1
    Mu_r = np.mean(Res_dist*Res)
    Mu_l = np.mean(DL_dist*DL + LL_dist*LL)
    Std_r = np.std(Res_dist*Res)
    Std_l = np.std(DL_dist*DL + LL_dist*LL)
    Cov_r = Std_r/Mu_r
    Cov_l = Std_l/Mu_l
    RI = math.log(Mu_r/Mu_l)/(math.sqrt((Cov_r**2) + (Cov_l**2)))

    plot_x.append(LL_ratio)
    plot_y.append(RI)
    LL_ratio = round(LL_ratio + 0.2, 2)

plt.plot(plot_x, plot_y, 'b-', lw=2, alpha=0.6, label='phi= '+str(mat))

plt.plot([0, 5], [3, 3], 'r--', lw=2, alpha=0.6, label='Target Reliability')
plt.legend(loc='best', frameon=False)
plt.title('Reliability Indices For DL + LL')
plt.xlabel("L/D Ratio")
plt.ylabel("Reliability Indices")
plt.axis([0, 5, 0, 5])
plt.show()

```

